

ENERGY MINIMIZATION IN PETLYUK DISTILLATION COLUMN

A DISSERTATION

*Submitted in partial fulfillment of the
requirements for the award of the degree*

of

MASTER OF TECHNOLOGY

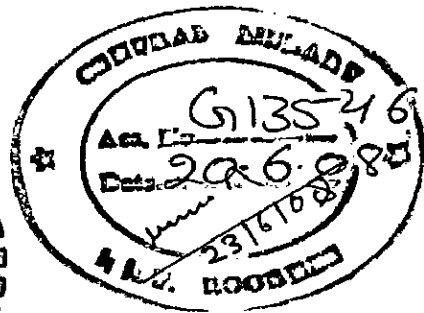
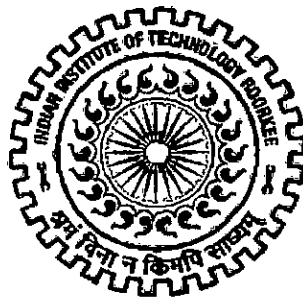
in

CHEMICAL ENGINEERING

(with specialization in Computer Aided Process Plant Design)

By

ASHOK KUMAR



**DEPARTMENT OF CHEMICAL ENGINEERING
INDIAN INSTITUTE OF TECHNOLOGY ROORKEE
ROORKEE - 247 667 (INDIA)
JUNE, 2007**

CANDIDATE'S DECLARATION

I hereby declare that the work which is being presented in the project entitled **"ENERGY MINIMIZATION IN PETLYUK DISTILLATION COLUMN"**, in partial fulfillment of the requirement for the award of the degree of Master of Technology in *Chemical Engineering with specialization in Computer Aided Process Plant Design*, submitted in the **Department of Chemical Engineering, Indian Institute of Technology Roorkee**, is an authentic record of my own work carried out during the period from July 2006 to June 2007, under the guidance **Dr. V.K. Agarwal**, Associate Professor, Department of Chemical Engineering, Indian Institute of Technology Roorkee.

The matter embodied in this project work has not been submitted for the award of any other degree.

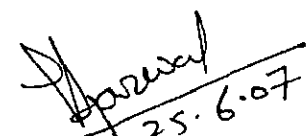
Date: June 25, 2007.

Place: IIT Roorkee.


(ASHOK KUMAR)

CERTIFICATE

This is to certify that the above statement made by the candidate is correct to the best of my knowledge.


(Dr. V.K. AGARWAL)
Associate Professor,
Department of Chemical Engineering,
Indian Institute of Technology-Roorkee.

ACKNOWLEDGEMENT

The few lines of acknowledgement can never substitute the deep appreciation that I have for all those without whose help, support and inspiration this dissertation would not have taken its present shape.

I wish to express my sincere thanks and sense of gratitude to my project guide, Dr. V. K. Agarwal, for his scholarly guidance, encouragement and discussion for this report. I am grateful to Dr. Shri Chand, HOD, Department of Chemical Engineering, IIT Roorkee, for providing me the necessary facilities for the compilation of this report.

I am indebted to all my colleagues, especially Vikas and Shyam for their immense help and motivation in carrying out the literature survey and computational work related to this report.

I extend warm appreciation to Mohd. Atif, Alok Sharma and Raghvendra Singh for their indispensable help in the completion of this work. The Library In-charge, Mrs. Verma, also deserve special thanks for placing the library at my disposal whenever required.

I am thankful to Mr. Siraj Alam for their unparalleled help and cooperation.

This report saw the light of the day only due to the encouragement and unflinching support and love of my parents, sisters and brothers.

Utmost thanks are due to the Almighty, for providing me the knowledge and wisdom for the successful completion of this report.

(ASHOK KUMAR)

ABSTRACT

Distillation is the most widely used industrial separation technology and distillation units are responsible for a significant part of the total heat consumption in the world's process industry. The reduction of energy consumption in distillation has become a need of the hour.

In this work we focus on Petlyuk distillation column for separation of multicomponent mixtures. The general analytic solution has been derived for minimum energy consumption in Petlyuk distillation column for multicomponent mixtures and the derivation is based on Underwood's classical methods. The V_{min} -diagram has been introduced as a useful tool for assessment of any multicomponent separation task. The total required energy consumption and the vapor load and separation carried out in all parts in a directly integrated column arrangement (i.e. Petlyuk Column) can be obtained by just a glance at the V_{min} -diagram.

Two extra degree of freedom can be used in Petlyuk distillation column for optimization purposes. The concept of self-optimizing control has been used for control structure design and in particular to propose that should be controlled to a set point and at the same time, this ensures close to optimal operation. We have studied the some performance of some self-optimizing control configurations for the Petlyuk column in the presence of disturbances and uncertainties.

It has been calculated, energy saving of 36% is achieved for ternary mixture of methanol, isopropanol and n-propanol with a Petlyuk distillation column, as compared to conventional distillation arrangements.

TABLE OF CONTENTS

CHAPTER	PAGE No.
CANDIDATE'S DECLARATION AND CERTIFICATE	i
ACKNOLEGEMENT	ii
ABSTRACT	iii
CONTENTS	iv
LIST OF FIGURES	vii
LIST OF TABLES	ix
NOMENCLATURE	x
1. INTRODUCTION	1
1.1 Petlyuk distillation Column	2
1.2 Objective of Present Study	3
2. LITERATURE SURVEY	4
2.1 Operation of Petlyuk Distillation Column	4
2.2 Optimization strategy for Petlyuk distillation Column	9
2.2.1 Energy Optimization in the Petlyuk Column	10
2.2.2 Optimizing Control Requirement for the Petlyuk Column	11
2.3 Underwood Equations for Minimum Energy in multi component distillation	12
2.3.1 Basic Definition	12
2.3.2 Definition of Underwood Roots	13
2.3.3 Underwood Roots for Minimum Vapor Flow	14
2.4 Vmin Diagram(Minimum Energy Mountain)	15

2.4.1	Feasible Flow Rates in Distillation	16
2.4.2	Binary Case	16
3.	MINIMUM ENERGY FOR THREE PRODUCTS PETLYUK ARRANGEMENTS	18
3.1	Brief Description of the Underwood Equations	18
3.2	The V_{min} – Diagram for Conventional Columns	19
3.3	The Underwood Equation Applied to the Petlyuk Column Prefractionator	20
3.3.1	Carry Over Underwood Roots in Thermally Coupled Columns	21
3.3.2	Minimum Energy of a ternary Petlyuk arrangement	24
3.3.2.1	Coupling Column C22 with Column C21 and C1	24
3.3.2.2	Visualization in the V_{min} Diagram	26
3.4	Computational Procedure	28
3.4.1	Algorithm to draw the V_{min} – Diagram	30
4.	SELF OPTIMIZING CONTROL FOR PETLYUK DISTILLATION COLUMN	31
4.1	Energy Optimization in Petlyuk Distillation Column	32
4.2	Self Optimizing control For the Petlyuk Column	34
4.3	Selecting Control Variables for Optimal Operation	34
4.3.1	The Performance Index (Cost) J	34
4.3.2	Open Loop Implementation	36
4.3.3	Closed Loop Implementation	37
4.3.4	A Procedure for Output Selection	39
4.4	Local Taylor Series Analysis	40
4.4.1	Expansion of the Cost Function	41
4.4.2	The Optimal Input	42
4.4.3	Expansion of Loss Function	43

5. RESULTS AND DISCUSSIONS	45
5.1 Model Validation	45
5.1.1 Case Study-I: Four Components Feed (ABCD)	48
5.1.2 Case Study-II: Ternary Feed (ABC)	50
5.2 Parameter Study	52
5.2.1 Variation in V_{min} at Different Composition of More Volatile Component (Methanol)	52
5.2.2 Variation in V_{min} by Changing Feed Conditions	59
6. CONCLUSIONS AND RECOMMENDATIONS	64
6.1 Conclusions	64
6.2 Recommendations	65
6.2.1 Process Design	65
6.2.2 Control Structure Design	65
6.2.3 Advanced Control	65
REFERENCES	67
APPENDIX-A	70

LIST OF FIGURES

Figure No.	Title	Page No.
Fig. 1.1	The Petlyuk Distillation Arrangement.	2
Fig. 2.1	Sketch of Petlyuk Distillation Column	5
Fig. 2.2	Relevant Variables for the Design of the Petlyuk System	9
Fig. 2.3	The V_{min} – Diagram or minimum Energy Mountain (Visualization of the Regions Distributing Components for Binary Feed case)	15
Fig. 3.1	The V_{min} – diagram For Ternary Mixture ABC. The Components Which are Distributed to Both Ends are Indicated in Each Region, With Corresponding active Underwood Roots.	19
Fig. 3.2	The Prefractionator of Petlyuk Arrangement	20
Fig. 3.3	Fully Thermally Coupled Column	21
Fig. 3.4	V_{min} – Mountain Diagram for a Ternary Feed Mixture (ABC)	26
Fig. 4.1	Fully Thermally Coupled Column	32
Fig. 4.2	Loss as a Function of Disturbances for Open Loop and Closed Loop Operation	39
Fig. 4.3	Optimal Control Move	43
Fig. 5.1	V_{min} – Diagram for the Ternary Mixture of Methanol, Isopropanol and n- Propanol	47
Fig. 5.2	V_{min} – Diagram for the Case Study-I: Four Components Feed	49
Fig. 5.3	V_{min} – Diagram for the Case Study-II: Ternary Mixture	51
Fig. 5.4	V_{min} – Diagram for the Ternary Mixture of Methanol, Isopropanol and n- Propanol at the Feed Composition of [0.1, 0.4, 0.5]	53
Fig. 5.5	V_{min} – Diagram for the Ternary Mixture of Methanol, Isopropanol and n- Propanol at the Feed Composition of [0.2, 0.2, 0.6]	54
Fig. 5.6	V_{min} – Diagram for the Ternary Mixture of Methanol, Isopropanol and n- Propanol at the Feed Composition o	

	[0.4, 0.4, 0.2]	55
Fig. 5.7	V _{min} – Diagram for the Ternary Mixture of Methanol, Isopropanol and n- Propanol at the Feed Composition of [0.7, 0.2, 0.1]	56
Fig. 5.8	V _{min} – Diagram for the Ternary Mixture of Methanol, Isopropanol and n- Propanol at the Feed Composition of [0.85, 0.1, 0.05]	57
Fig. 5.9	Comparison of Minimum Vapor Flow Requirement in Sharp A/B and Sharp B/C Split With Respect to Composition of More Volatile Component (Methanol)	58
Fig. 5.10	V _{min} – Diagram for Cold Ternary Mixture of Methanol, Isopropanol and n- Propanol at the Feed Composition of [0.3, 0.3, 0.4]	59
Fig. 5.11	V _{min} – Diagram for Saturated Liquid Mixture of Methanol, Isopropanol and n- Propanol at the Feed Composition of [0.3, 0.3, 0.4]	60
Fig. 5.12	V _{min} – Diagram for Partly Vapor Mixture of Methanol, Isopropanol and n- Propanol at the Feed Composition of [0.3, 0.3, 0.4]	61
Fig. 5.13	V _{min} – Diagram for Saturated Vapor Mixture of Methanol, Isopropanol and n- Propanol at the Feed Composition of [0.3, 0.3, 0.4]	62
Fig. 5.14	V _{min} – Diagram for Superheated Vapor Mixture of Methanol, Isopropanol and n- Propanol at the Feed Composition of [0.3, 0.3, 0.4]	63

LIST OF TABLES

Table No.	Title	Page No.
Table.5.1	Vapor Flow Rates at the Peaks and Knots in the Vmin Diagram for Ternary Mixture of Methanol, Isopropanol and n-Propanol (For Model Validation).	46
Table. 5.2	Vapor Flow Rates at the Peaks and Knots in the Vmin Diagram for Case Study-I: Four Products Separation	48
Table. 5.3	Vapor Flow Rates at the Peaks and Knots in the Vmin Diagram for Case Study-II	50
Table. A.1	Vapor Flow Rates at the Peaks and Knots in the Vmin Diagram at Different Composition of the Saturated Liquid Feed.	70
Table. A.2	Vapor Flow Rates at the Peaks and Knots in the Vmin Diagram at Different Feed Conditions.	71

NOTATION AND NOMENCLATURE

It is attempted to define the notation used for equations in the text. However, the most important nomenclature used for distillation columns are summarized:

V	Vapour flow rate
L	Liquid flow rate
D, B, S	Product flows (, or net flow ($D=V-L$))
W_i	Net component flow through a section (positive upwards)
r_i	Feed component recovery
R_V	Vapour split ratio at vapour draw stage
R_L	Liquid split ratio at liquid draw stage
x	Mole fraction in liquid phase
y	Mole fraction in vapour phase
z	Mole fraction in feed
q	Liquid fraction (feed quality)
A, B	Component enumeration
T	Temperature
P	Pressure
p_i	Partial pressure of component i
p^o	Vapour pressure
α	Relative volatility, referred to a common reference component
ϕ	Underwood root in a top section
ψ	Underwood root in a bottom section
Θ	Common (minimum energy) Underwood root

- λ Specific heat of vaporization
- ΔH Enthalpy change
- ΔS Entropy change
- R The universal gas constant (8.31 J/K/mole)

Superscripts

Cxy Column address in a complex arrangement: column array number x, array row number y. unless it is obvious from the context, the column position is given as the first superscript to the variables. The column address may be omitted for the first column (C1)

i/j Denotes sharp split between components i and j.

Subscripts

T, B....., Top or bottom section

F, D, B, S.... Streams

min Minimum energy operation for a given column feed

i, j, A, B.... Component enumeration

CHAPTER 1

INTRODUCTION

As the distillation columns call for energy consumption and huge capital outlays, the reduction of energy consumption in distillation has become a need of the hour. This work is focus on directly (fully thermally) coupled column arrangements for separation of multicomponent mixtures. These systems are also denoted Petlyuk arrangements, where a particular implementation is the dividing wall column. An important motivation for studying integrated distillation column arrangements is to reduce the energy consumption. On a global basis, distillation columns consume a large portion of the total industrial heat consumption, so even small improvements which become widely used, can save huge amounts of energy. Savings in the magnitude of 30-40% reboiler duty can be obtained if a three-product integrated Petlyuk column is operated at its optimum, instead of using a conventional column sequence. In addition to energy savings, such integrated units have also a potential for reduced capital cost, making them extra attractive.

From the point of view of energy requirements, separation sequences using conventional columns (a single feed with two product streams, condenser and reboiler) suffer from an inherent inefficiency produced by the thermodynamic irreversibility during the mixing of streams at the feed, top and bottom of the column. This remixing is inherent to any separation that involves an intermediate boiling component. This inefficiency can be improved by removing some heat exchangers and introducing thermal coupling between columns. If a heat exchanger is removed the liquid reflux (or vapor load) is provided by a new stream that is withdrawn from another column, in this way it is possible to reduce the energy consumption and under some circumstances also the capital costs. A Petlyuk distillation configuration is reached when the entire vapor load is provided by a single reboiler and all the reflux by a single condenser.

1.1 Petlyuk Distillation Column

This is the structural arrangement which shows an interconnection between two columns with a liquid or vapor extraction from the first column and the recycle stream from the other column in the other phase; such interconnection can be implemented in place of reboiler or a condenser of one of the columns. The Petlyuk distillation configuration has received considerable attention because of its efficiency to reduce the energy required for the separation of ternary mixtures.

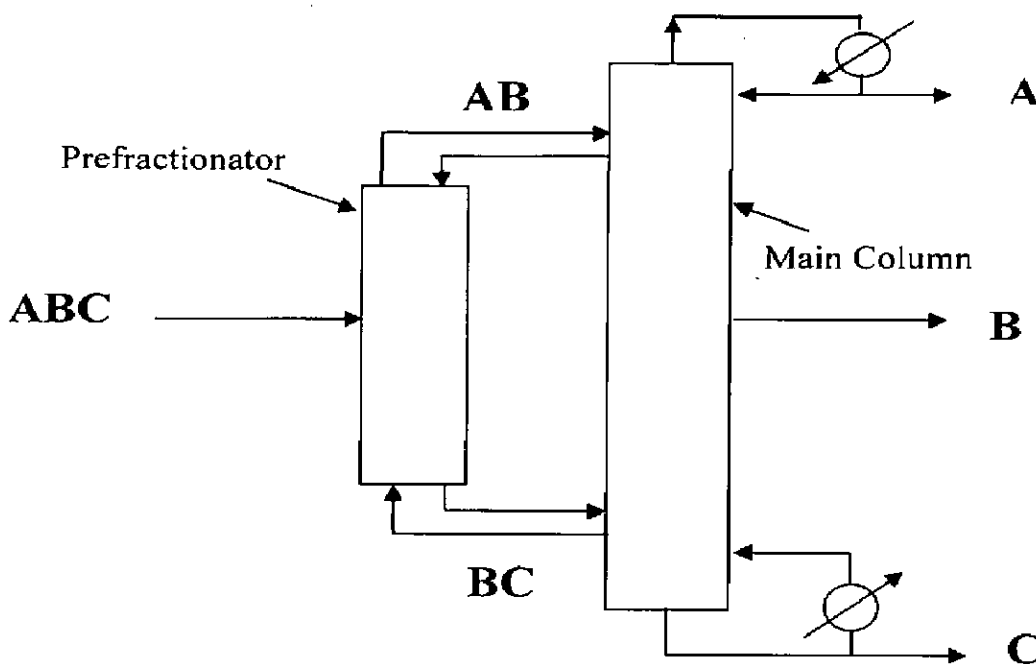


Fig. 1.1: The Petlyuk Distillation Arrangement.

The main features of Petlyuk distillation column are:-

1. No more than one component is stripped out in each section, key components A and C:
 - Reversibility during mixing of streams in feed location (pinch zone)
 - No remixing effect
2. Thermal coupling:
 - No thermodynamic losses in heat exchanges of prefractionator reboiler and condenser
 - Reversibility during mixing of streams at ends of columns.

3. Large potential for reduced energy consumption:
 - Savings of 30-40% reboiler duty can be achieved for 3-product Petlyuk columns compared to conventional column sequences.

1.2 Objective of Present Study

The present investigation is planned to address the following objectives:

- Formation of Underwood's classical equations for minimum energy.
- Derive the general analytic solution for minimum energy consumption in Petlyuk distillation column for multicomponent feed and any number of products.
- Use of the graphical tool (V_{\min} diagram) for visualization of minimum energy related feed distribution.
- Self optimizing control of Petlyuk distillation column using local Taylor series analysis by turning the optimization problem into a constant setpoint problem.

CHAPTER 2

LITERATURE SURVEY

Distillation columns are the most widely used separation units in the petrochemical and chemical industries. In order to reduce their significant energy consumption there has been several successful developments by the use of process and energy integration techniques. A possible way is the integration of conventional distillation columns into the remainder of the process. If this integration is limited or impossible, the operation of the distillation columns should be investigated and/ or energy-integrated solutions between the individual columns and nonconventional arrangements should be considered such as Petlyuk distillation arrangement, heat integration and thermocoupling. The aim of these energy-integrated schemes is cost saving by less energy consumption. The successful schemes are usually compared to the conventional arrangements as well as to other energy-integrated alternatives. The selection from the several energy-integrated solutions is usually based on economic features. The Petlyuk distillation configuration has received considerable attention because of its efficiency to reduce the energy required for the separation of ternary mixtures. But the structure of the Petlyuk system offers some control challenges arising from the transfer of vapor streams back and forth between the columns.

2.1 Operation of Petlyuk Distillation Column:

Alstad et. al [2] showed that for Petlyuk distillation columns, it may be optimal from an energy point of view, to over-fractionate one of the product streams. Additional energy savings may also be possible when bypassing some of the feed and mixing it with the over-fractionated product stream. However, it should be noted that the distillate product will contain component *C* which may be undesirable. These results have been confirmed numerically for the case with finite number of stages, where it is optimal to over-fractionate the non-limiting section as expected. This implies that one may either

choose to over-fractionate (in operation) or decrease the number of stages in the non limiting section (design).

The Petlyuk distillation column (Fig.2.1), with a pre-fractionator (C1) and a main column (C21 and C22), is an interesting alternative to the conventional cascade of binary columns for separation of ternary mixtures. The potential savings are reported to be of approximately 30% in both energy and capital cost.

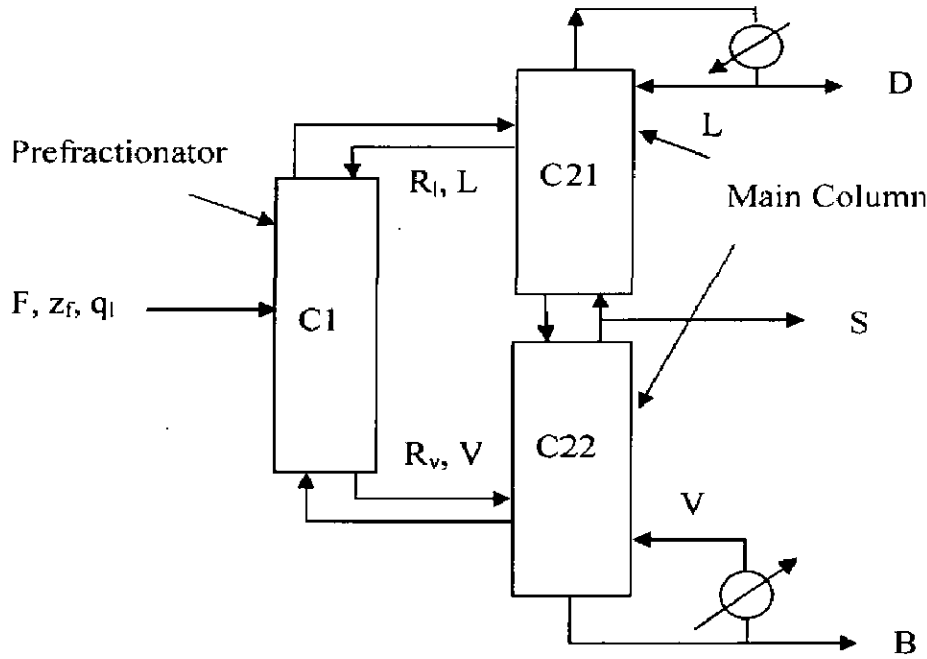


Fig. 2.1: Sketch of Petlyuk distillation column

Halvorsen and Skogestad (2003) calculated the vapor flows by following expressions for minimum energy:

$$V_{T,\min}^{C21} = \frac{\alpha_A W_{A,T}^{C21}}{\alpha_A - \theta_A} + \frac{\alpha_B W_{B,T}^{C21}}{\alpha_B - \theta_A} = D \left[\frac{\alpha_A x_{A,D}}{\alpha_A - \theta_A} + \frac{\alpha_B (1 - x_{A,D})}{\alpha_B - \theta_A} \right] \quad (2.1)$$

$$V_{B,\min}^{C22} = \frac{\alpha_B W_{B,B}^{C22}}{\alpha_B - \theta_B} + \frac{\alpha_C W_{C,B}^{C22}}{\alpha_C - \theta_B} = -B \left[\frac{\alpha_A (1 - x_{C,B})}{\alpha_A - \theta_B} + \frac{\alpha_B x_{C,B}}{\alpha_B - \theta_B} \right] \quad (2.2)$$

Kim, Y.H. [13], was presented structural design procedure for fully thermally coupled distillation columns (FTCDC) is applied to the example system of butanol isomers in order to show the design performance. The procedure gives structural

information of the column, and therefore iterative computation encountered in the design using conventional procedure and commercial packages can be eliminated. Using the outcome of the structural design, other topics, such as thermodynamic efficiency, dividing wall column structure and the arrangement of interlinking streams, are investigated. Finally, a 3×3 operation scheme, which has favorable indices of multivariable controllability, is examined by checking the control performances of set-point tracking and regulation with a model predictive control.

For the side product is drawn from a main column in fig.2.1, the design of the column begins with the composition of the product. Starting at the stage of side product, the liquid composition at one stage above the product stage is computed using the composition of the product and an equilibrium relation:

$$x_{n+1,i} = \frac{K_{n,i} x_{n,i}}{\sum_j K_{n,j} x_{n,j}} \quad (2.3)$$

Where K_{ni} is equilibrium constant of the i th component at the n th tray from the bottom and obtained from an equilibrium relation. This procedure continues until the tray composition meets the specification of overhead product. The liquid composition of the stages below the side product stage is found in the same manner and the composition equation is modified as (2.4):

$$x_{n-1,i} = \frac{x_{n,i}}{K_{n-1,i} \sum_j \left(\frac{x_{n,j}}{K_{n-1,j}} \right)} \quad (2.4)$$

In order to analyze the operational characteristic of an FTCDC, its dynamic simulation is conducted in which the change of operation variables is applied and examined the variation of product composition. The initial operation condition of the dynamic simulation is derived from the design result of the previous section.

The liquid composition is updated from the material balance of a component in a tray:

$$Mn \frac{dx_{n,i}}{dt} = L_{n+1}x_{n+1,i} + V_{n-1}y_{n-1,i} - L_n x_{n,i} - V_n y_{n,i} \quad (2.5)$$

A structural design procedure for fully thermally coupled distillation columns is exercised to an example system having different compositions of feed. The structural information from the design eliminates tedious iteration encountered in the design using conventional procedures. From the result of the design for the example system and the comparison of calculated liquid composition with a commercial design tool, it is proved that the proposed procedure is useful. In addition, other design related subjects, such as thermodynamic efficiency, dividing wall structure and the arrangement of interlinking streams, are investigated using the information of the structural design and possible improvements concerning the subjects are suggested. Mixing in feed tray reduces the thermodynamic efficiency more than the remixing of intermediate component. A separate prefractionator system is better than the dividing wall structure unless the concentrations of intermediate component in feed and side product are close. For the column operation, a 3×3 control scheme is adopted and its performance of set-point tracking and regulation with a model predictive control is examined to result in satisfactory outcome.

Halvorsen et al [18] computed important operational parameters for an infinite-staged Petlyuk column as a function of the feed composition, feed enthalpy, and relative volatilities. The computational effort is very low, and the methods can be used to quickly evaluate the applicability of a Petlyuk column for a specific separation task. It is found that the largest energy savings of about 40% are obtained when the prefractionator is operated at its preferred split and the feed composition is such that both the upper and lower parts of the main column operate at their respective minimum reflux condition. The position of this boundary region relative to the actual feed is very important when we consider important operational aspects of the column.

The minimum boilup rate for the Petlyuk column is given by:

$$V_{\min}^{\text{Petlyuk}} = \max \left(\frac{\alpha_B z_B}{\theta_A - \alpha_B} + \frac{\alpha_C z_C}{\theta_A - \alpha_C}, \frac{\alpha_C z_C}{\theta_B - \alpha_C} \right) \quad (2.6)$$

The Underwood roots (θ_A, θ_B) obey $\alpha_A > \theta_A > \alpha_B > \theta_B > \alpha_C$ and can be found by solving eq. (2.7)

$$\frac{\alpha_A z_A}{\alpha_A - \theta} + \frac{\alpha_B z_B}{\alpha_B - \theta} + \frac{\alpha_C z_C}{\alpha_C - \theta} = (1 - q) \quad (2.7)$$

The minimum vapor flow for the prefractionator for a sharp A/C split is given by

$$V_{1,\min}(\beta) = \max \left(\frac{\alpha_A z_A}{\alpha_A - \theta_A} + \frac{\alpha_B z_B \beta}{\alpha_B - \theta_A}, \frac{\alpha_A z_A}{\alpha_A - \theta_B} + \frac{\alpha_B z_B \beta}{\alpha_B - \theta_B} \right) \quad (2.8)$$

Simple analytical Underwood methods developed for the infinite-staged Petlyuk column with a sharp product split can be used to compute the theoretical performance of a Petlyuk arrangement for any set of feed properties and operational situations. For every set of feed parameters and relative volatilities, the full surface $V(R_1, R_V)$ can easily be computed and analyzed. We observe that the best possible energy savings is obtained close to the feed composition region, where the operating point for the preferred split of the prefractionator coincides with the situation that we have the same minimum reflux requirement in the upper and lower parts of the main column, i.e., when the main column is balanced. This region is also the most difficult region for operation because we have to adjust both degrees of freedom online. However, if the feed composition is away from the boundary line, then optimal operation (in terms of minimum boilup) can be obtained with a strategy where one of the degrees of freedom, e.g., the vapor split, is kept constant. The results shown in this paper are valid for sharp product splits and therefore relevant for high-purity distillation. A typical symptom of a real column if we have a feed composition outside the feasible regions for high-purity operation is that we will be unable to produce high-purity products, even if the energy input to the column is above the theoretical minimum. So, instead of an increase in the energy consumption for non optimal operation, we may experience decreasing product purity, particularly in the side stream.

2.2 Optimization strategy for Petlyuk distillation Column:

Hernandez *et al* [10] reported that the dynamic model is based on the total mass balance, component mass balances, equilibrium relationship (ideal VLE), summation constraints, energy balance, and stage hydraulics (Francis Weir formula). One set of equations must be written for each column of the Petlyuk system. The equations are coupled because of the two recycle streams between the columns; therefore, the full set of equations must be solved simultaneously. An important aspect for the design of the system is the specifications of the two recycle streams, a liquid stream that leaves column C-2 from stage NR and enters at the top of column C-1, and a vapor stream that leaves column C-2 from stage NS2 and constitutes the feed stream at the bottom of column C-1 (Fig. 2.2). We define the following dimensionless variables for these streams, which lie between 0 and 1 and are used as search variables in the optimization procedure:

$$\eta_V = \frac{V_B}{V_{NS2}} \quad (2.9)$$

$$\eta_L = \frac{L_T}{L_{NR}} \quad (2.10)$$

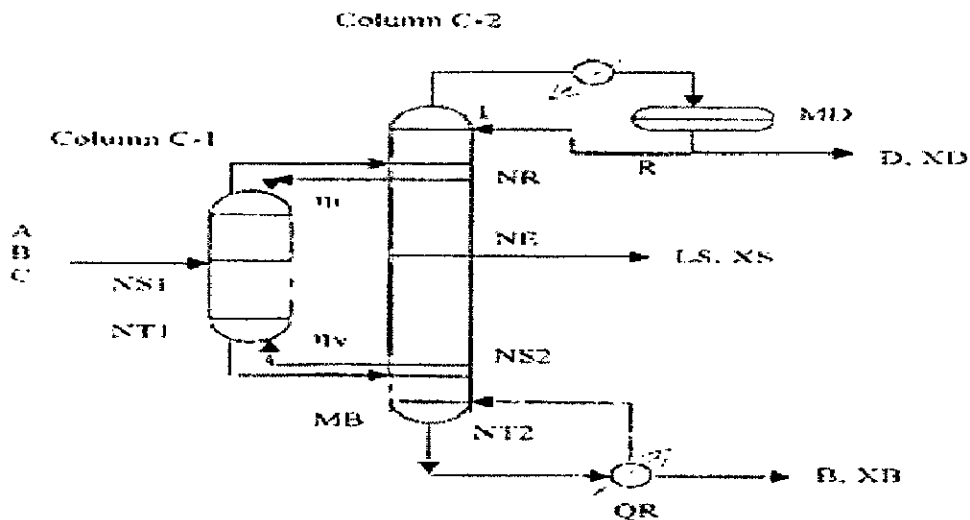


Fig. 2.2 Relevant variables for the design of the Petlyuk system.

The dynamic model requires a basic structure of the Petlyuk system. Such a preliminary design can be obtained by the shortcut method of *Triantafyllou and Smith (1992)*, or through the implementation of some expected distribution of the intermediate component. The dynamic model serves two purposes. First, it will detect whether the proposed design can effectively provide the desired products compositions, and secondly it will identify the operating conditions under which minimum energy consumption will be achieved. The following steps are used for the optimization procedure.

1. Specify products compositions for the Petlyuk system. These values are taken as set points for the dynamic model.
2. Establish the control loops between each manipulated variable (R , LS and QR) and its corresponding output variable (XD , XS and XB).
3. Set a value for η_V .
4. Set a value for η_L .
5. Initialize time to start the rigorous dynamic simulation.
6. Integrate the dynamic model (*Hernandez & Jimenez, 1996*).
7. Compare product compositions with set point values. If they do not agree, increase time by Δt and go back to step 6. If they agree, a search point is completed; the operating values for R , LS and QR are detected.
8. Increase η_L and go back to step 5 until the local minimum of heat duty is detected.
9. Increase η_V and go back to step 4 until the overall minimum of heat duty is found.

It is important to note that an adjustment of the initial design might be needed if the final steady state compositions do not agree with the established set points.

2.2.1 Energy Optimization in the Petlyuk Column

Serra et. al [7] studied that the thermally coupled distillation column known as Petlyuk column (Petlyuk 1965), shown in figure 2.1, is a complex distillation arrangement to separate a ternary mixture of A (the more volatile), B (intermediate volatility) and C (the less volatile). The Petlyuk column has been given special attention due to very high reported energy savings. (*Triantafyllou and Smith, 1992*) reported savings of 30% comparing the Petlyuk column with the conventional trains of columns.

The complex design of the Petlyuk column offers some extra degrees of freedom which permit an optimization that is not possible in the conventional ternary distillation designs.

2.2.2 Optimizing Control Requirement for the Petlyuk Column

Halvorsen et. al (1996) assumed that the Petlyuk column reboiler and accumulator levels are stabilized by the distillate flow (D) and the bottoms flow (B). Then it has five degrees of freedom: boilup (V), reflux (L), side stream flow (S), liquid split (R_l) and vapor split (R_v). Of these five degrees of freedom, three are used to control the compositions of the three products (composition of component A in the distillate, composition of B in the side stream and composition of C in the bottoms stream). (Wolff and Skogestad, 1996) showed that the LSV control structure give acceptable performance. It consists in the control of A composition by the reflux (L), the control of the B composition by the side stream flow (S) and the control of C composition by the boilup (V). LSV is the control structure assumed in this work. Therefore, liquid split (R_l) and vapour split (R_v) are the two extra variables to be used for optimization purposes. The energy consumption, here represented by the boilup vapour rate (V) will be used as the criterion. When the composition loops are closed and the products purity are controlled to their specifications, the product specifications setpoints will replace the composition control loop inputs (L, S and V), as degrees of freedom. These setpoints will affect the optimal operation point in addition to the disturbances in the feed flow rate (F), feed composition (z) and feed liquid fraction (q).

It was shown (*Halvorsen and Skogestad, 1997, 1998*) that the optimal operation point of the Petlyuk column is not robust when no optimizing control is applied in addition to the product composition control. The optimal values of the two degrees of freedom (R, R_v) used for optimization are sensitive to feed disturbances and product set points changes. The objective function surface $V(R_l, R_v)$ is very steep in some directions and if no adjustment of these remaining degrees of freedom (DOF) is applied, the operation may get far from optimal. Therefore, some control is required to maintain the optimal operation when disturbances and uncertainties are present. However, in accordance with the work of (*Halvorsen and Skogestad, 1998*), we will fix R_v and use R_l as the only manipulated variable to indirectly achieve the energy control. Two reasons

justify this decision. First the energy surface $V(R_l, R_v)$ is quite flat close to the minimum in a narrow long region in a certain direction in the (R_l, R_v) -plane, permitting that for any given R_v , can find a $R_{l,opt,1}$ that makes the value of $V(R_{l,opt,1}, R_v)$ be close to the absolute minimum when both values of the remaining DOFs are optimized: $V(R_{l,opt}, R_{v,opt})$. R_v must be set in a reasonable neighborhood to $R_{v,opt}$. The flat region was shown by (Fidkowski 1986) for infinite stages and sharp product splits. The extent of the flat region is determined by the feed properties (composition and liquid fraction), and the relative volatility of the components. Second, if we consider a dividing wall column (DWC) (Wright 1949), R_v would be a difficult variable to manipulate in normal operation since its value will be naturally given by the pressure equalization on each side of the dividing wall.

2.3 Underwood Equations for Minimum Energy in multi-component distillation

2.3.1 Basic Definition:

The starting point for Underwood's methods for multicomponent mixtures is the material balance equation at a cross section in the column. The net material transport (W_i) of component i upward through a stage n is the difference between the amount traveling upward from a stage as vapor and the amount entering a stage from above as liquid:

$$W_i = V_n y_{i,n} - L_{n+1} x_{i,n+1} \quad (2.11)$$

Note that at steady state W_i is constant through each column section. In the following, Skogestad *et. al* [8] assumed constant molar flows ($L = L_n = L_{n-1}$ and $V = V_n = V_{n+1}$) and constant relative volatility (R_i).

The vapor-liquid equilibrium (VLE) at an equilibrium stage is given by:

$$y_i = \frac{\alpha_i x_i}{\sum_{i=1}^{N_c} \alpha_i x_i} \quad (2.12)$$

In the top section, the net product flow is $D = V_n - L_{n+1}$ and

$$W_{i,T} = x_{i,D} D = r_{i,D} z_i F \quad (2.13)$$

In the bottom section, $B = L_{n+1} - V_n$, and the net material flow is

$$W_{i,B} = -x_{i,B} B = r_{i,B} z_i F \quad (2.14)$$

The positive direction of the net component flows is defined upward, but in the bottom the components normally travel downward from the feed stage and then we have $W_{i,B} \leq 0$. With a single feed stream, the net component flow in the feed is given as

$$W_{i,F} = z_i F \quad (2.15)$$

A recovery can then be regarded as a normalized component flow:

$$r_i = \frac{W_i}{W_{i,F}} = \frac{W_i}{z_i F} \quad (2.16)$$

At the feed stage, $W_{i,F}$ is defined as positive into the column.

2.3.2 Definition of Underwood Roots:

The Underwood roots (ϕ) in the top section are defined as the N_c solutions of

$$V_T = \sum_{i=1}^{N_c} \frac{\alpha_i W_{i,T}}{\alpha_i - \phi} \quad (2.17)$$

In the bottom there is another set of Underwood roots ψ given by the solutions of

$$V_B = \sum \frac{\alpha_i W_{i,B}}{\alpha_i - \psi} \quad (2.18)$$

Equations (2.17) & (2.18) are related via the material balance at the feed stage:

$$W_{i,T} - W_{i,B} = W_{i,F} = z_{i,F}F \quad (2.19)$$

The change in vapor flow at the feed stage given by the liquid fraction (q) of the feed (F)

$$V_F = V_T - V_B = (1 - q)F \quad (2.20)$$

Computation of the Underwood roots involves solving a straightforward polynomial root problem, but make sure that the vector of component flows W_T or W_B is feasible. This also implies that in the multicomponent case there is a “hidden” interaction between the unspecified elements in W_T and the Underwood roots.

2.3.3 Underwood Roots for Minimum Vapor Flow

Underwood showed a series of properties of the roots (ϕ and ψ) for a two-product column with a single reboiler and condenser. In this conventional column, all components flow upward in the top section ($W_{i,T} \geq 0$) and downward in the bottom section ($W_{i,B} \leq 0$). With N_c components there are, for each of ϕ and ψ , N_c solutions obeying

$$\alpha_1 > \phi_1 > \alpha_2 > \phi_2 > \alpha_3 > \phi_3 \dots \dots \dots > \alpha_{N_c} > \phi_{N_c} \quad (2.21)$$

$$\psi_1 > \alpha_1 > \psi_2 > \alpha_2 > \psi_3 > \alpha_3 \dots \dots \dots > \psi_{N_c} > \alpha_{N_c} \quad (2.22)$$

Recall that $V_T - V_B = (1 - q)F$. By subtracting the defining equations for the top and bottom sections (2.17) and (2.18), we obtain the following equation, which is valid for the common roots only (denoted θ):

$$(1 - q) = \sum_i \frac{\alpha_i z_i}{\alpha_i - \theta} \quad (2.23)$$

We will denote a root θ_K an *active* root for the case when $\phi_K = \psi_{K+1} = \theta_K$. Inserting the active root in the top- and bottom-defining equations gives the minimum flow for a given set of component distributions.

$$V_{T,\min} = \sum_i \frac{\alpha_i W_{i,T}}{\alpha_i - \theta_K} \quad \text{or} \quad V_{T,\min} = \sum_i \frac{\alpha_i r_{i,T} z_i F}{\alpha_i - \theta_K} \quad (2.24)$$

2.4 V_{\min} Diagram (Minimum-Energy Mountain)

A nice feature, because there are only 2 degrees of freedom, is that we can visualize the entire operating range in two dimensions, even with an arbitrary number of feed components. We choose to use (a) vapor flow per unit feed (V/F) and (b) product split, expressed by the distillate (D/F), as degrees of freedom. The choice of vapor flow rate on the ordinate provides a direct visualization of the energy consumption and column load. We chose to use the vapor flow in the top (V_T) on the ordinate when the feed quality $q \neq 1$.

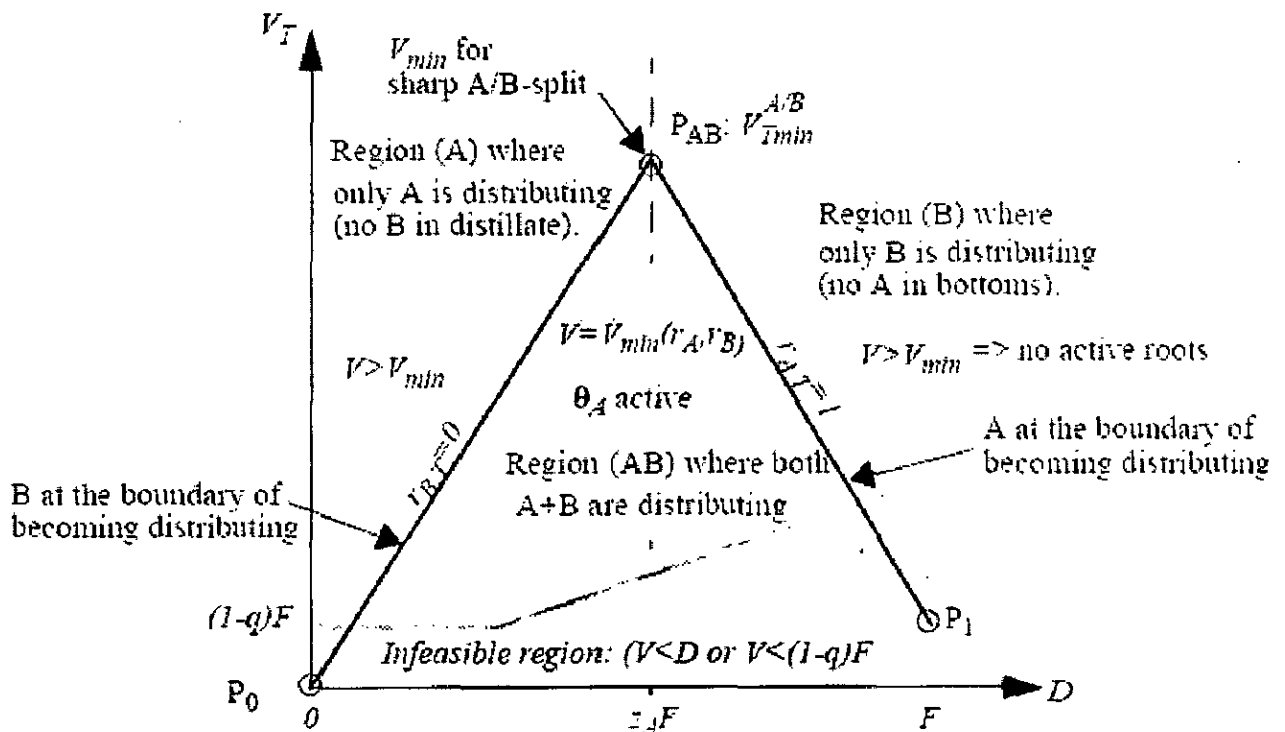


Fig. 2.3 The V_{\min} -diagram, or minimum energy mountain (Visualization of the regions distributing components for a binary feed case).

2.4.1 Feasible Flow Rates in Distillation

The D - V plane spans out the complete feasible operating space for the column, both the minimum energy solutions and all others. This is quite simple to understand from an operational viewpoint. D and V_T are just flows, and we can operate a column with any feasible combination of flows through the separation stages. If we alternatively specify two key component recoveries as degrees of freedom, we can only span a sub-region of the operating space, and we do not know in advance if our specification is feasible. Feasibility simply implies that we require positive vapor and liquid flows in all sections:

$$V_T > 0, V_B > 0, L_T > 0, L_B > 0 \quad (2.25)$$

In an ordinary two product column we also require $D = V_T - L_T \geq 0$ and $B = L_B - V_B \geq 0$ (note that this is not a feasibility requirement for directly coupled sections) which with a single feed translates

$$\text{to } V_T = \max \left((1 - q)F, D \right) \quad \text{and} \quad 0 \leq \frac{D}{F} \leq 1 \quad (2.26)$$

2.4.2 Binary Case

Consider a feed with light component A and heavy component B with relative volatilities $[\alpha_A, \alpha_B]$, feed composition $z = [z_A, z_B]$, feed flow rate $F=1$ and liquid fraction q . In this case we obtain from the feed equation (3.23) a single common root Θ_A obeying $\alpha_A > \Theta_A > \alpha_B$. The minimum vapor flow is found by applying this root in the definition equation (3.24):

$$\frac{V_{T \min}}{F} = \frac{\alpha_A r_{A,T} z_A}{\alpha_A - \theta_A} + \frac{\alpha_B r_{B,T} z_B}{\alpha_B - \theta_A} \quad (2.27)$$

If we want to specify the product split as one degree of freedom, we introduce D/F as an extra variable and the following extra equation:

$$\frac{D}{F} = \sum r_{i,T} z_i = r_{A,T} z_A + r_{B,T} z_B \quad (2.28)$$

We obtain the following results which we plot in the in the D - V -plane of the V_{min} diagram in Figure 2.3 First we find the operating point which gives sharp A/B-split

$$P_{AB} : [r_{A,T}, r_{B,T}] = [0,0] \Rightarrow [D, V_{T,min}] = [0,0]$$

and then the asymptotic points:

$$P_O : [r_{A,T}, r_{B,T}] = [0,0] \Rightarrow [D, V_{T,min}] = [0,0]$$

$$P_1 : [r_{A,T}, r_{B,T}] = [1,1] \Rightarrow [D, V_{T,min}] = [1, (1-q)]F$$

These three points make up a triangle as shown in Figure 3. Along the straight line P_O - P_{AB} we have $V=V_{min}$ for a pure top product ($r_{B,T} = 0$), and the line can be expressed by:

$$\frac{V_T}{F} = \frac{\alpha_A r_{A,T} z_A}{\alpha_A - \theta_A} \text{ where } D = r_{A,T} z_A F \quad (2.29)$$

Similarly, along the straight line P_{AB} - P_1 , we have $V=V_{min}$ for a pure bottom product ($r_{A,T} = 1$), and the line can be expressed by:

$$\frac{V_T}{F} = \frac{\alpha_A z_A}{\alpha_A - \theta_A} + \frac{\alpha_B r_{B,T} z_B}{\alpha_B - \theta_B} \text{ where } \frac{D}{F} = z_A + r_{B,T} z_B \quad (2.30)$$

Above the triangle (V_{min} -mountain), $V > V_{min}$ and we have no active Underwood roots, so (3.27) no longer applies. However, since only one component is distributing, we have either $r_{A,T} = 1$ or $r_{B,T} = 0$. This implies that the recoveries are directly related to D , and we have:

$$\frac{D}{F} = r_{A,T} z_A \text{ for } \frac{D}{F} \leq z_A \text{ or } \frac{D}{F} = z_A + r_{B,T} z_B \text{ For } \frac{D}{F} \geq z_A \quad (2.31)$$

Anywhere above the triangle we obviously waste energy since the same separation can be obtained by reducing the vapour flow until we hit the boundary to region AB. $V_T > D$ and $V_T > (1-q)F$ for feasible operation of a conventional two-product distillation column. The shaded area represents an infeasible region where a flow rate somewhere in the column would be negative.

CHAPTER 3

MINIMUM ENERGY FOR THREE PRODUCTS PETLYUK ARRANGEMENTS

3.1 Brief Description of the Underwood Equations

Consider a two-product distillation column with a multicomponent feed (F) with liquid fraction q and composition vector z of N components. The defining equation for the Underwood roots (ϕ) in the top and (ψ) in the bottom are:

$$\text{Top: } V_T = \sum_{i=1}^N \frac{\alpha_i W_{i,T}}{\alpha_i - \phi} \quad \text{Bottom: } V_B = \sum_{i=1}^N \frac{\alpha_i W_{i,B}}{\alpha_i - \psi} \quad (3.1)$$

There will be N solutions for each root and the sets from the top and bottom equations are generally different. Note that the net flow for a component (W_i) is defined positive upwards, also in the bottom. Underwood showed that with infinite number of stages, minimum vapor flow is obtained when pairs of roots in the top and bottom coincide. By subtracting the equations above, we obtain what we denote the feed equation, which gives us the set of possible common roots Θ :

$$V_T - V_B = \sum_{i=1}^N \frac{\alpha_i (W_{i,T} - W_{i,B})}{\alpha_i - \theta} = \sum \frac{\alpha_i z_i F}{\alpha_i - \theta} = (1 - q)F \quad (3.2)$$

Underwood showed, that for ordinary columns, the number of each set of roots is equal to number of components (N), and they obey: $\alpha_i > \phi_i > \Theta_i > \psi_{i+1} > \alpha_{i+1}$, and that the $(N-1)$ possible common roots are in the range between all volatilities. When we apply the material balance at the feed stage, we observe that the possible common roots depend only on feed composition and quality, and not on how the column is operated. However, it is not obvious when we may apply the common roots back into the defining equations, in particular for more than binary mixtures. The general rule is that we may apply the common roots being in the range of volatilities for the components distributed to both ends. We denote these roots active roots. If we have any active roots

then $V = V_{min}$ and there will be a unique solution for a given product purity specification, Otherwise $V > V_{min}$.

We assumed that constant pressure and constant relative volatilities, and then the vapor liquid equilibrium (VLE) relationship between the vapor (y) and liquid (x) compositions is given by:

$$y_i = \frac{\alpha_i x_i}{\sum_{j=1}^N \alpha_j x_j} \quad (3.3)$$

3.2 The V_{min} -diagram for Conventional Columns

Since a two-product column operated at constant pressure has only two degrees of freedom we may visualize all possible operating points in the D-V plane. This is illustrated in the V_{min} -diagram, which is shown for a ternary feed (with components ABC) in Figure 3.1. The diagram provides an informative visualization of the exact solutions for any given set of feasible specifications and infinite number of stages.

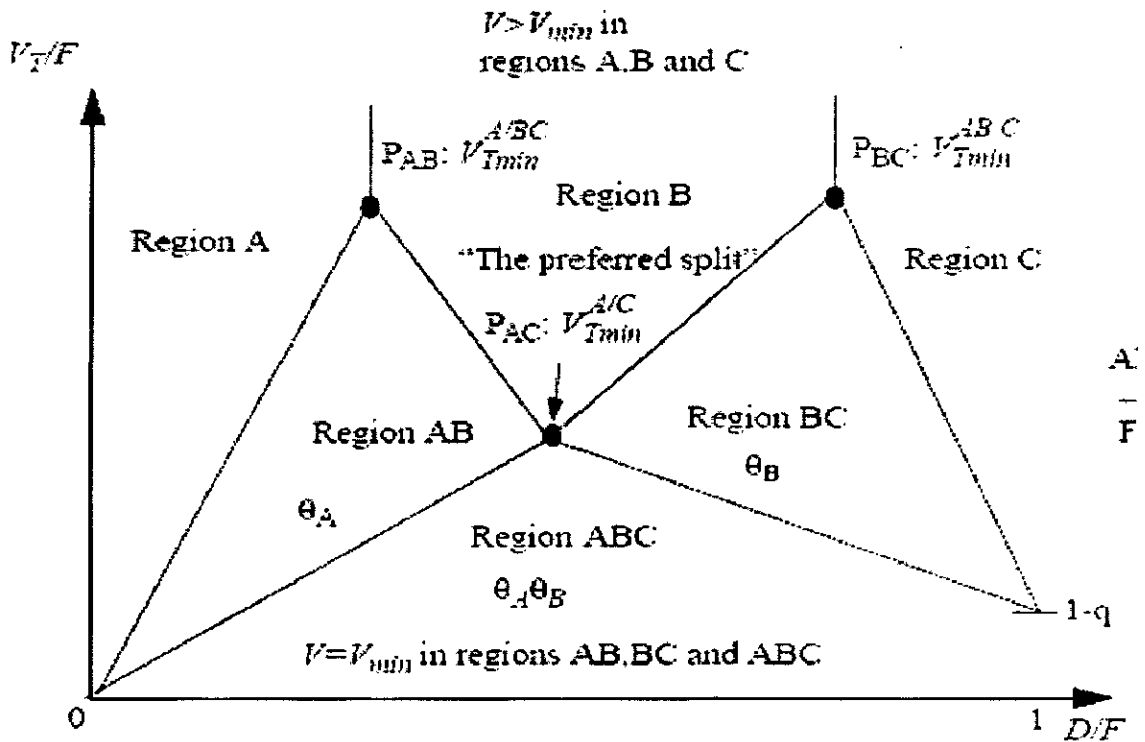


Fig. 3.1 The V_{min} -diagram for a ternary mixture ABC. The components which are distributed to both ends are indicated in each region, with the corresponding active Underwood roots.

Each peak or knot in this diagram (P_{ij}) is the operating point for minimum vapor flow and sharp split between the component pair i,j ($V_{min}^{i,j}$). The straight lines between the peaks and knots are a distribution boundary where a component is at the limit of appearing or disappearing in one of the product streams. We denote the distribution regions by the components being distributed to both products when operating in that region. For example in region AB components A and B are distributing to both products, whereas component C only appear in the bottom product. In region A, B and C we have no common Underwood roots and $V > V_{min}$. Below the "mountain", in regions AB, ABC or BC, one or more pair of Underwood roots coincide and $V = V_{min}$. The actual active common roots are those in the range between the volatilities of the distributing components.

3.3 The Underwood Equations Applied to the Petlyuk Column Prefractionator

In the prefractionator of a Petlyuk column we can still use the net component flow (w) or feed recovery (r) to describe the separation carried out in the column. From the material balance at any cross-section in the column:

$$W_{i,n} = V_n y_{i,n} - L_{n+1} x_{i+1,n} \quad (3.4)$$

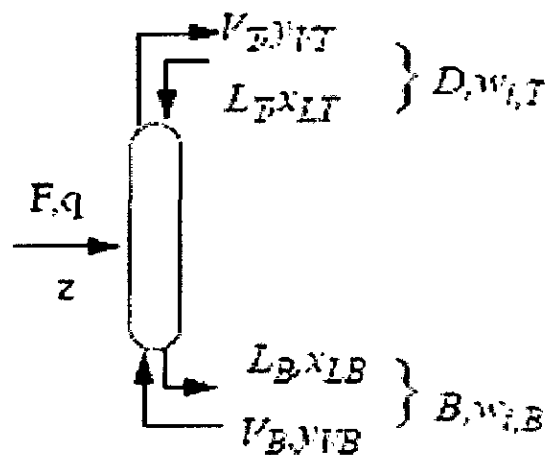


Fig. 3.2 The prefractionator of a Petlyuk Arrangement

Thus, for the column in Figure 3.2 the composition in the flow leaving the column top is dependent on the composition of the incoming flow through the material balance:

$$y_{i,VT} = \frac{W_{i,T} + L_T x_{i,LT}}{V_T} \quad (3.5)$$

For a conventional column with total condenser $x_{i,LT} = y_{i,VT}$, and we have a unique relation between net component flow and the product composition for a given distillate flow: $y_{i,VT} L_T = W_{i,T} / D$, where $D = V_T - L_T$.

We may regard the vapor flow entering the Petlyuk column prefractionator at the bottom and the liquid flow entering at the top as independent feeds with compositions (x_{LT}, y_{VB}) . Thus the number of degrees of freedom in operation is now increased, because in addition to L_T and V_B we may also consider the new "end-feed" compositions (x_{LT}, y_{VB}) as degrees of freedom.

The Underwood equations used to produce the V_{min} -diagram have been deduced from the material balance (3.4) and the vapor liquid equilibrium, without considering product compositions at all. However, that the results are based on the restrictions $W_{i,T} \geq 0$ and $W_{i,B} \leq 0$. In a conventional column, these conditions are always fulfilled, but the prefractionator in Figure 2.3 may be operated in modes where these restrictions are not met. Thus provided these restrictions are fulfilled, the equations behind the V_{min} -diagram will also apply for the Petlyuk column prefractionator.

3.3.1 Carry Over Underwood Roots in Directly Coupled Columns

The vapor flow in the top of the prefractionator is given by the Underwood defining equation:

$$V_T^{C1} = \sum_i \frac{\alpha_i W_{i,T}^{C1}}{\alpha_i - \phi^{C1}} \quad (3.6)$$

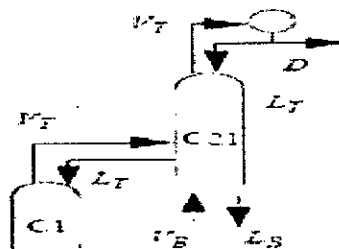


Fig.3.3 Fully Thermally Coupled Column (Petlyuk Column)

The top and bottom defining equations for column C21 become:

$$V_T^{C21} = \sum_i \frac{\alpha_i W_{i,T}^{C21}}{\alpha_i - \phi^{C21}} \quad \text{and} \quad V_B^{C21} = \sum_i \frac{\alpha_i W_{i,B}^{C21}}{\alpha_i - \psi^{C21}} \quad (3.7)$$

The material balance at the connection point gives:

$$V_T^{C21} - V_B^{C21} = V_T^{C1} \quad \text{and} \quad W_{i,T}^{C21} - W_{i,B}^{C21} = W_{i,T}^{C1} \quad (3.8)$$

The combination of these gives the feed equation for column C21 where the common roots (Θ^{C21}) appear:

$$V_T^{C21} - V_B^{C21} = \sum_i \frac{\alpha_i (W_{i,T}^{C21} - W_{i,B}^{C21})}{(\alpha_i - \theta^{C21})} = \sum_i \frac{\alpha_i W_{i,T}^{C1}}{(\alpha_i - \theta^{C21})} = V_T^{C1} \quad (3.9)$$

Here we observe that the feed equation of column C21 (3.9) is identical to the top section defining equation for column C1 in (3.6). Thus the possible common roots in column C21 are equal to the actual roots from the defining equation in the top of column C1:

$$\theta^{C21} = \phi^{C1} \quad (3.10)$$

The common roots (Θ) of column C1 are found from the feed equation for the main feed (note that we will omit the superscript C1 for column C1), which with a ternary is the familiar expression:

$$\frac{\alpha_A z_A}{\alpha_A - \theta} + \frac{\alpha_B z_B}{\alpha_B - \theta} + \frac{\alpha_C z_C}{\alpha_C - \theta} = (1 - q) \quad (3.11)$$

Since an active common root represents a minimum vapor solution in a single column, and $\Theta^{C21} = \phi^{C1}$, we have the following relation for the ternary feed example where we recover all of the light component in the top of C21 with the middle and

heavy component recovery equal to zero:

$$\frac{V_T^{C21}}{F} = \frac{\alpha_A z_A}{\alpha_A - \phi_A^{C21}} \geq \frac{\alpha_A z_A}{\alpha_A - \theta_A^{C21}} = \frac{\alpha_A z_A}{\alpha_A - \phi_A^{C1}} \geq \frac{\alpha_A z_A}{\alpha_A - \theta_A^{C1}} \quad (3.12)$$

This implies the following relation for the roots:

$$\theta_A^{C1} \leq \phi_A^{C1} = \theta_A^{C21} \leq \phi_A^{C21} \quad (3.13)$$

The minimum vapor flow in column C21 for any given operation of C1 is when the common root in C21 is active. Then for the first root $\phi_A^{C21} = \theta_A^{C21} = \phi_A^{C1}$ and

$$\frac{V_{T \min}^{C21}}{F} = \frac{\alpha_A z_A}{\alpha_A - \phi_A^{C1}} \quad (3.14)$$

The absolute minimum solution is found when ϕ_A^{C1} is equal to the common root ($\theta_A^{C1} = \theta_A$). Then the common root of C1 becomes active in both columns at the same time ($\phi_A^{C21} = \theta_A^{C21} = \phi_A^{C1} = \theta_A^{C1}$):

$$\min_{C1} \left(\frac{V_{T \min}^{C21}}{F} \right) = \frac{\alpha_A z_A}{\alpha_A - \theta_A} \quad (3.15)$$

We may generalize this expression to any number of components and feasible recoveries in the top with the following equation set (one equation for each root $\theta_k \in [\theta_1, \dots, \theta_{N_{dT}^{C21}-1}]$ given by the N_{dT}^{C21} components distributed to the top of C21):

$$\min_{C1} \left(\frac{V_{T \min}^{C21}}{F} \right) = \sum \frac{\alpha_i z_i r_{i,T}^{C21}}{(\alpha_i - \theta_k^{C1})} \quad (3.16)$$

The relation in (3.12) also shows that any sub-optimal operation of either column C1 or C21 cannot be recovered by the other. The operation of both has to be optimized simultaneously to achieve the overall minimum vapor flow in C21 as in (3.16).

For a column C22 connected to the bottom of column C1, we will find equivalent results. For the ternary feed case, with full recovery of the heavy component C in the bottom of column C22 and middle and light component recovery is equal to zero, the equivalent to equation (3.15) becomes:

$$C1 \left(\frac{V_{B \min}^{C22}}{F} \right) = \frac{-\alpha_C z_C}{\alpha_C - \theta_B} = \frac{\alpha_A z_A}{\alpha_A - \theta_B} + \frac{\alpha_B z_B}{\alpha_B - \theta_B} - (1 - q) \quad (3.17)$$

We have not considered the actual compositions in the junction streams. However, we know that the composition in the return flow into the top of C1 has no influence on the product split in C1 unless a component which would have been removed in a conventional prefractionator were to be introduced in that return flow. This implies that for nonsharp operation of C1, (where all components distribute and all common roots are active) the return flow composition has no influence at all. For referred split operation, this is also true when we ensure that there is no heavy(C) component in the return flow. In normal operation regimes of C1 and C21, the conditions are trivially fulfilled. This is very important and somewhat surprising because from a glance at a Petlyuk arrangement, we might expect all kinds of complicated recycle effects due to the two-way flows in the direct coupling.

3.3.2 Minimum Energy of a Ternary Petlyuk Arrangement

3.3.2.1 Coupling Column C22 with Columns C21 and C1

Now we have the necessary background to deduce the simple analytical solution for minimum vapor flow in the Petlyuk arrangement as shown in Figure 3.1. For sharp A/C split in column C1 and sharp A/B split in column C21, minimum vapour flow requirement in the top of C21 is given by equation (3.14):

$$V_T^{C21} \geq V_{T \min}^{C21} = \frac{\alpha_A z_A}{\alpha_A - \phi_A^{C1}} F \quad (3.18)$$

We can also find the equivalent for the bottom flow in C22 for sharp B/C split from equation (3.17):

$$V_B^{C22} \geq V_{B \min}^{C22} = \frac{-\alpha_C z_C}{\alpha_C - \psi_C^{C1}} \quad (3.19)$$

Due to the direct coupling we know that the absolute minimum vapour flow in C21 is found when we operate column C1 in a region where $\phi_A = \Theta_A$. Similarly, the absolute minimum for vapour flow in C22 is found when C1 is operated in a region where $\psi_C = \Theta_B$. For sharp product splits, the preferred split is the only point of operation where both common roots carry over to C21 and C22 at the same time. Any other solution will give a larger value for the minimum vapour flow in at least one of C21 or C22 so we know that we really only have to consider the solution at preferred split operation of C1. Now we relate these expressions to the required vapour flow in the bottom reboiler of the Petlyuk arrangement:

$$V_{B \min}^{Petlyuk} = \max(\min(V_{T \min}^{C21}) - (1-q)F, \min(V_{B \min}^{C22})) \quad (3.20)$$

For sharp product splits, we can express this as:

$$V_{B \min}^{Petlyuk} = \max\left(\frac{\alpha_A z_A}{\alpha_A - \theta_A} - (1-q), \frac{-\alpha_C z_C}{\alpha_C - \theta_B}\right)F \quad (3.21)$$

We may use the feed equation (3.11) to remove the feed quality term $(1-q)F$ from the Underwood expressions, as we have done in (3.22). In addition we here relate the minimum vapor flow to the top condenser:

$$V_{T \min}^{Petlyuk} = V_{B \min}^{Petlyuk} + (1-q)F = \max\left(\frac{\alpha_A z_A}{\alpha_A - \theta_A}, \frac{\alpha_A z_A}{\alpha_A - \theta_B} + \frac{\alpha_B z_B}{\alpha_B - \theta_B}\right)F \quad (3.23)$$

This minimum solution implies that either C21 or C22 may get a vapour flow larger than its minimum value. However, this only affects the local behavior of that column, and not the product composition and the operation of the prefractionator and the other column. The reason is that, although the composition in the connection point to the prefractionator may be altered and in theory might influence the separation in the

prefractionator, the product composition has no influence on the recovery of feed components unless a removed component is reintroduced, or there is a reverse flow of components back into the column. Thus we have to verify that the heavy C cannot reach the feed junction to C21 and that the light A cannot reach the feed junction to C22 in the main column.

3.3.2.2 Visualization in the V_{min} - diagram

Figure 3.4 show an example of the V_{min} -diagram, or “minimum energy mountain” for a ternary feed (ABC).

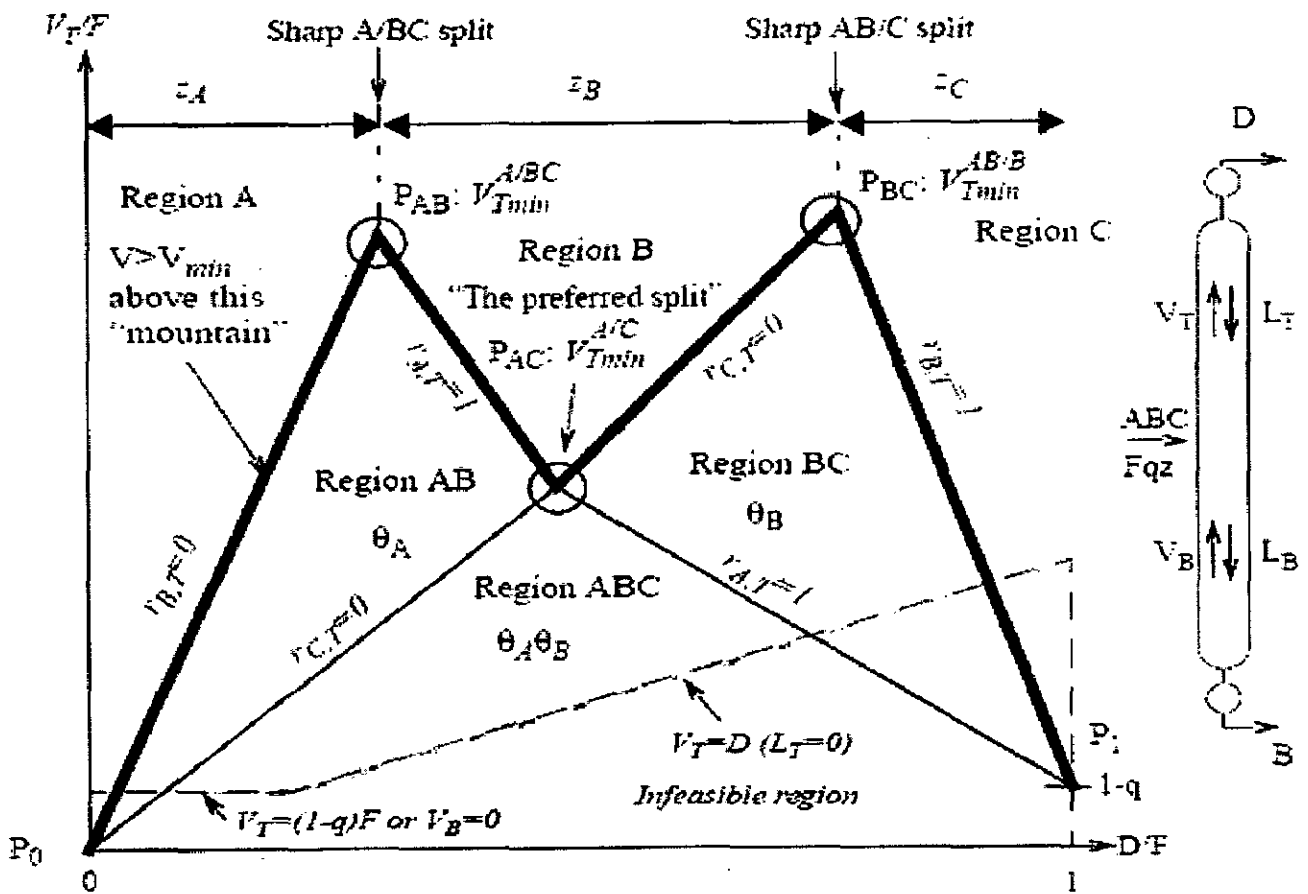


Fig. 3.4 V_{min} -“mountain”-diagram for a ternary feed mixture (ABC). $V > V_{min}$ above the solid “mountain” P_0 - P_{AB} - P_{AC} - P_{BC} - P_1 . Below this boundary $V = V_{min}$ for all cases, but the distribution of feed components to the product are dependent on operating region. These regions are denoted AB, BC and ABC from the distributing components. The active roots are also indicated.

The peaks, which give V_{\min} for sharp splits A/B and B/C (no distributing components):

$$P_{AB} : [r_{A,T}, r_{B,T}] = [1,0] \Rightarrow [D, V_{T \min}] = \left[z_A, \frac{\alpha_A z_A}{\alpha_A - \theta_A} \right] F$$

$$P_{BC} : [r_{B,T}, r_{C,T}] = [1,0] \Rightarrow [D, V_{T \min}] = \left[(z_A + z_B), \frac{\alpha_A z_A}{\alpha_A - \theta_B} + \frac{\alpha_B z_B}{\alpha_B - \theta_B} \right] F$$

The preferred split, which gives V_{\min} for sharp A/C – split (B is distributing):

$$P_{AC} : [r_{A,T}, r_{C,T}] = [1,0] \Rightarrow [D, V_{T \min}] = \left[(z_A + \beta z_B), \frac{\alpha_A z_A}{\alpha_A - \theta_B} + \frac{\alpha_B \beta z_B}{\alpha_B - \theta_B} \right] F$$

$$\beta = r_{B,T}^{A/C} = - \frac{\alpha_A z_A (\alpha_B - \theta_A)(\alpha_B - \theta_B)}{\alpha_B z_B (\alpha_A - \theta_A)(\alpha_A - \theta_B)}$$

Where β is the recovery of B:

And the trivial asymptotic points:

$$P_0 : [r_{A,T}, r_{B,T}] = [0,0] \Rightarrow [D, V_{T \min}] = [0,0]$$

$$P_1 : [r_{A,T}, r_{B,T}] = [1,1] \Rightarrow [D, V_{T \min}] = [1, (1 - q)]F$$

The two peaks (PAB and PBC) give us the minimum vapour flow for sharp split between A/B and B/C, respectively. The valley, PAC, gives us the minimum vapour flow for a sharp A/C split and this occurs for a specific distribution of the intermediate component B, known as the “preferred split”.

A part of the V_{\min} -boundary, namely the V-shaped PAB-PAC-PBC curve, has been illustrated by several authors, e.g. Fidkowski (1986), Christiansen and Skogestad (1997). It gives the minimum vapour flow for a sharp split between A and C as a function of the distillate flow. Figure 3.4, gives the complete picture for all feasible operating points. In every region where more than one component may be distributing to both products (AB, BC and ABC), at least one Underwood root is active.

3.4 COMPUTATIONAL PROCEDURE

Consider a set of N_d distributing components, denoted: $\{d_1, d_2, \dots, d_{Nd}\}$. The recoveries in the top are trivially $r_{i,T} = 1$ for all non-distributing light components ($i < d_1$), and $r_{i,T} = 0$ for the non-distributing heavy components ($i > d_{Nd}$). Then, with a given distribution set we know the $N_c - N_d$ recoveries of the non-distributing components.

Then we use another of Underwood's results: For any minimum vapour flow solution, the active Underwood roots will only be those with values in the range between the volatilities of the distributing components ($\alpha_{d1} > \Theta_k > \alpha_{dNd}$). This implies that with N_d distributing components, the number of active roots is:

$$N_a = N_d - 1 \quad (3.24)$$

Define the vector X containing the recoveries of the N_d distributing components and the normalized vapor flow in the top section:

$$X = \left[r_{d1,T}, r_{d2,T}, \dots, r_{dNd,T}, \frac{V_T}{F} \right]^T \quad (3.25)$$

(Superscript T denotes transposed). The equation set (2.24) can be written as a linear equation set on matrix form:

$$M \bullet X = Z \quad (3.26)$$

With the detailed elements in the matrices expanded, this is same as:

$$\begin{bmatrix} \frac{\alpha_{d1}z_{d1}}{\alpha_{d1} - \theta_{d1}} & \frac{\alpha_{d2}z_{d2}}{\alpha_{d2} - \theta_{d1}} & \dots & \frac{\alpha_{dNd}z_{dNd}}{\alpha_{d1} - \theta_{d1}} & -1 \\ \frac{\alpha_{d1}z_{d1}}{\alpha_{d1} - \theta_{d2}} & \frac{\alpha_{d2}z_{d2}}{\alpha_{d2} - \theta_{d2}} & \dots & \frac{\alpha_{dNd}z_{dNd}}{\alpha_{d1} - \theta_{d2}} & -1 \\ \dots & \dots & \dots & \dots & -1 \\ \frac{\alpha_{d1}z_{d1}}{\alpha_{d1} - \theta_{dNd-1}} & \frac{\alpha_{d2}z_{d2}}{\alpha_{d2} - \theta_{dNd-1}} & \dots & \frac{\alpha_{dNd}z_{dNd}}{\alpha_{d1} - \theta_{dNd-1}} & -1 \end{bmatrix} \bullet \begin{bmatrix} r_{d1,T} \\ r_{d2,T} \\ \dots \\ r_{dNd} \\ V_T / F \end{bmatrix} = \begin{bmatrix} -\sum_{i=1}^{d1-1} \frac{\alpha_i z_i}{\alpha_i - \theta_{d1}} \\ -\sum_{i=1}^{d1-1} \frac{\alpha_i z_i}{\alpha_i - \theta_{d2}} \\ \dots \\ -\sum_{i=1}^{d1-1} \frac{\alpha_i z_i}{\alpha_i - \theta_{dNd-1}} \end{bmatrix}$$

The elements in each column of M arise from the term in (2.24) related to the distributing components, and we have one row for each active root. Z contains the part

of (2.24) arising from the non-distributing light components with recovery one in the top. The recoveries for the heavy non-distributing components are zero in the top, so these terms disappear.

There are $N_{\bar{a}}=N_{d-1}$ equations (rows of M and Z) and N_{d+1} variables in X (columns in M). Thus by specifying any two of the variables in X as our degrees of freedom we are left with N_{d-1} unknowns which can be solved from the linear equation set in (3.25).

If we want to specify the product split as one degree of freedom, we introduce D/F as an extra variable and the following extra equation:

$$D/F = \sum r_{i,T} z_i \quad (3.27)$$

Then the linear equation set (5.2) can be expanded to give:

$$\begin{bmatrix} \frac{\alpha_{d1} z_{d1}}{\alpha_{d1} - \theta_{d1}} & \frac{\alpha_{d2} z_{d2}}{\alpha_{d2} - \theta_{d1}} & \dots & \frac{\alpha_{dNd} z_{dNd}}{\alpha_{d1} - \theta_{d1}} & -1 & 0 \\ \frac{\alpha_{d1} z_{d1}}{\alpha_{d1} - \theta_{d2}} & \frac{\alpha_{d2} z_{d2}}{\alpha_{d2} - \theta_{d2}} & \dots & \frac{\alpha_{dNd} z_{dNd}}{\alpha_{d1} - \theta_{d2}} & -1 & 0 \\ \dots & \dots & \dots & \dots & -1 & 0 \\ \frac{\alpha_{d1} z_{d1}}{\alpha_{d1} - \theta_{dNd-1}} & \frac{\alpha_{d2} z_{d2}}{\alpha_{d2} - \theta_{dNd-1}} & \dots & \frac{\alpha_{dNd} z_{dNd}}{\alpha_{d1} - \theta_{dNd-1}} & -1 & 0 \\ z_{d1} & z_{d2} & \dots & z_{dNd} & 0 & -1 \end{bmatrix} \cdot \begin{bmatrix} r_{d1,T} \\ r_{d2,T} \\ \dots \\ r_{dNd} \\ V_T / F \\ D/F \end{bmatrix} = \begin{bmatrix} -\sum_{i=1}^{d1-1} \frac{\alpha_i z_i}{\alpha_i - \theta_{d1}} \\ -\sum_{i=1}^{d1-1} \frac{\alpha_i z_i}{\alpha_i - \theta_{d2}} \\ \dots \\ -\sum_{i=1}^{d1-1} \frac{\alpha_i z_i}{\alpha_i - \theta_{dNd-1}} \\ -\sum_{i=1}^{d1-1} z_i \end{bmatrix} \quad (3.28)$$

The problem of finding the correct distribution set is dependent on how we specify the two degrees of freedom. An example of a specification which always gives a feasible solution is $r_{LK,T} = 1$ and $r_{HK,T} = 0$. That is, when we want to find the minimum energy operation point for sharp split between a light key (LK) component in the top and a heavy key (HK) in the bottom. Then we always know that the common Underwood roots with values between the relative volatilities of the keys will be active, thus $d_1 = LK$ and $d_{Nd} = HK$ and the structure of equation (3.25) is thereby known.

3.4.1 Algorithm to Draw the V_{min} – mountain-diagram

The procedure for computing the required points to draw the V_{min} -mountain-diagram for a general multicomponent case (N_c components) is as follows:

1. Find all possible common Underwood roots $[\theta_1, \theta_2, \theta_3, \dots, \theta_{N_c - 1}]$ from the feed equation (2.23).
2. Use equation (3.28) to find the full solutions for sharp split between every possible pair of light (LK) and heavy key (HK) specifications. Each solution gives the component recoveries (R), minimum vapour flow (V_{min}/F) and product split (D/F). These are the peaks and knots in the diagram, and there are $N_c(N_c - 1)/2$ such key combinations, described in more detail below:
 - $N_c - 1$ cases with no intermediates (e.g. AB, BC, CD,...) These points are the peaks in the V_{min} -diagram
 - $N_c - 2$ cases with one intermediate (e.g. AC, BD, CE,...) These are the knots between the peaks, and the line segments between the peaks and these knots forms the V_{min} -boundary etc.
 - 2 cases with $N_c - 3$ intermediates ($N_c - 1$ components distribute)
 - 1 case with $N_c - 2$ intermediates (all components distribute)

This last case is the “preferred split” solution where the keys are the most light and heavy components, and all intermediates distribute.

3. Finally we will find the asymptotic points where all recoveries in the top are zero and one, respectively. These are trivially found as $V_{T,min}=0$ for $D=0$ and $V_{T,min}=(1-q)F$ for $D=F$.

Chapter 4

SELF-OPTIMIZING CONTROL FOR PETLYUK DISTILLATION COLUMN

In a Petlyuk distillation column, two extra degrees of freedom can be used for optimization purposes. It has been reported that a typical energy saving of 30 - 40 % is achievable with a Petlyuk distillation column, compared to conventional distillation arrangements. However, the optimal steady-state operation point can be difficult to maintain in practice. In this chapter we have studied the performance of some self-optimizing control configurations for the Petlyuk distillation column in presence of disturbances and uncertainties. The results show that self-optimizing control can be used to improve the robustness of optimal operation by adjusting a degree of freedom in a feedback control loop by keeping a suitable measurement variable at a setpoint.

Self-optimizing control is an approach to solve this problem by turning the optimization problem into a set point problem. The key idea is to find a measurable variable with constant value at optimal operation. If this variable can be found, a feedback control loop is closed to keep the variable at the set point, and to keep indirectly the process at optimal operation. Since self-optimizing control results in a feedback control loop, it will be robust against disturbances and model uncertainties compared to any open loop model based optimization methods. The application of self-optimizing control to the Petlyuk distillation column was already addressed in (Halvorsen and Skogestad, 1998). Some candidate measurable feedback variables for the Petlyuk distillation column were proposed and analyzed in a qualitative way. This work has to be seen as a continuation of that one in which a more careful evaluation is performed. New candidate feedback variables have been proposed and a quantitative study has been done to see the performance of the controlled system in face of various process disturbances and model uncertainties.

4.1 Energy optimization in Petlyuk Distillation Column

The thermally coupled distillation column known as Petlyuk column (Petlyuk 1965), shown in figure 4.1, is a complex distillation arrangement to separate a ternary mixture of A (the more volatile), B (intermediate volatility) and C (the less volatile). The Petlyuk column has been given special attention due to very high reported energy savings. (Triantafyllou and Smith, 1992) reported savings of 30% comparing the Petlyuk column with the conventional trains of columns. Considerable investment capital savings can be obtained if the arrangement is implemented in a single shell (Divided Wall Column). The complex design of the Petlyuk column offers some extra degrees of freedom which permit an optimization that is not possible in the conventional ternary distillation designs.

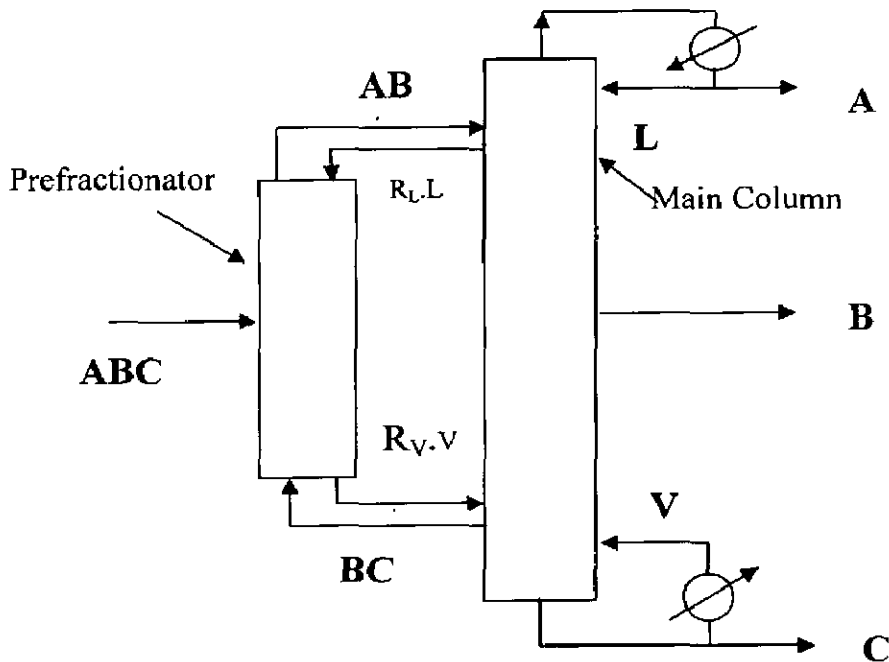


Fig. 4.1: Fully thermally Coupled Column

We assume that the Petlyuk column reboiler and accumulator levels are stabilized by the distillate flow (D) and the bottoms flow (B). Then it has five degrees of freedom: boilup (V), reflux (L), side stream flow (S), liquid split (R_L) and vapour split (R_V). Of these five degrees of freedom, three are used to control the compositions of the three products (composition of component A in the distillate, composition of B in the side stream and

composition of C in the bottoms stream). (Wolff and Skogestad, 1996) showed that the LSV control structure give acceptable performance. It consists in the control of A composition by the reflux (L), the control of the B composition by the side stream flow (S) and the control of C composition by the boilup (V). LSV is the control structure assumed in this work. Therefore, liquid split (R_L) and vapour split (R_V) are the two extra variables to be used for optimization purposes. The energy consumption, here represented by the boilup vapour rate (V) will be used as the criterion. When the composition loops are closed and the products purity are controlled to their specifications, the product specifications setpoints will replace the composition control loop inputs (L, S and V), as degrees of freedom. These setpoints will affect the optimal operation point in addition to the disturbances in the feed flow rate (F), feed composition (z) and feed liquid fraction (q).

It was shown (Halvorsen and Skogestad, 1997, 1998) that the optimal operation point of the Petlyuk column is not robust when no optimizing control is applied in addition to the product composition control. The optimal values of the two degrees of freedom (R_L , R_V) used for optimization are sensitive to feed disturbances and product set points changes. The objective function surface $V(R_L, R_V)$ is very steep in some directions and if no adjustment of these remaining degrees of freedom (DOF) is applied, the operation may get far from optimal. Therefore, some control is required to maintain the optimal operation when disturbances and uncertainties are present. However, in accordance with the work of (Halvorsen and Skogestad, 1998), we will fix R_V and use R_L as the only manipulated variable to indirectly achieve the energy control. Two reasons justify this decision. First the energy surface $V(R_L, R_V)$ is quite flat close to the minimum in a narrow long region in a certain direction in the (R_L, R_V)-plane, permitting that for any given R_V , we can find a $R_{L,opt,1}$ that makes the value of $V(R_{L,opt,1}, R_V)$ be close to the absolute minimum when both values of the remaining DOFs are optimized: $V(R_{L,opt}, R_{V,opt})$. R_V must be set in a reasonable neighborhood to $R_{V,opt}$. The flat region was shown by (Fidkowski 1986) for infinite stages and sharp product splits. The extent of the flat region is determined by the feed properties (composition and liquid fraction), and the relative volatility of the components.

4.2 Self-Optimizing Control for The Petlyuk Column

The concept of self-optimizing control is presented in (Skogestad et. al. 1998 and 1999). A brief introduction for our Petlyuk column case study will be given here. The idea behind self-optimizing control is to find a variable which characterize operation at the optimum, and the value of this variable at the optimum should be less sensitive to variations in disturbances than the optimal value of the remaining degrees of freedom. Thus if we close a feedback loop with this candidate variable controlled to a setpoint, we should expect that the operation will be kept closer to optimum when a disturbance occur. We define u to be our remaining degrees of freedom which we will use as manipulative variables for optimizing control, and d to include the external disturbances, the setpoint specifications for all the closed control loops and any remaining degrees of freedom not used as manipulative variables. In our general case $u = (R_L, R_V)$ and $d = (z, q, x_{DA}, x_{SB}, x_{BC})$, but when we fix R_V and use R_L as the only manipulative variable we will have $u = R$ and $d = (z, q, x_{DA}, x_{SB}, x_{BC}, R_V)$. The optimal solution is found by minimizing $V(u, d)$ with respect to u . Thus both the optimal value of the criterion function V_{opt} and the corresponding solution u_{opt} will be a function of d .

$$V_{opt}(d) = \min_u V(u, d) = V(u_{opt}(d), d) \quad (4.1)$$

The combined set of (u, d) determines an operation point uniquely, and also the values of any internal states and measurements. Assume now that we choose a measurement variable $c = g(u, d)$, and that the inverse function $u = g^{-1}(c, d)$ exists. Then we may apply $u = g^{-1}(c_s, d)$, where c_s is the setpoint.

4.3 Selecting Controlled Variables For Optimal Operation

4.3.1 The Performance Index (Cost) J

We assume that the optimal operation problem can be quantified in terms of a scalar performance index (cost) J , such that the objective of the operation is to minimize J with respect to the available degrees of freedom. J may be a purely economic objective, but is more generally a weighted sum of the various control objectives. For the optimization itself it does not really matter which variables we use as degrees of freedom as long as they form an independent set. Let the base set for the degrees of freedom be denoted u (these may consist,

for example, of a subset the physical manipulators m). In addition, the cost will depend on the unknown disturbances d (which here is assumed to include uncertainty in the model and uncertainty in the optimizer). We can then write $J(u,d)$. The nominal value of the disturbances is denoted d_0 , and we can solve the nominal operating problem and obtain $u_{opt}(d_0)$ for which:

$$J_{opt}(d) = \min_u J(u, d) = J_{opt}(u_{opt}(d), d) \quad (4.2)$$

From this we can obtain a table with the corresponding optimal value of any other dependent variable, including the optimal value of any measurement $C_{opt}(d_0)$.

The issue is now to decide how to best implement the optimal policy in the presence of uncertainty by selecting the right set of controlled variables c with constants setpoints $c_S = c_{opt}(d_0)$. Here it is assumed that the number of controlled variables y equals the number of independent variables u , or more exactly that we starting from $c=f(u, d)$ can derive the inverse relationship:

$$u = f^{-1}(c, d) \quad (4.3)$$

Where the function f^{-1} exists and is unique.

Instead of evaluating the mean value of the performance index, it may be better to evaluate the always positive loss function. The loss function expresses the difference between the actual operating costs (e.g. obtained when we adjust u in order to keep c at a given setpoint) and the optimal operating cost (obtained with $u=u_{opt}(d)$),

$$L(u, d) = J(u, d) - J_{opt}(d) \quad (4.4)$$

The objective of the operation is to minimize J , or equivalently to minimize the loss L . The loss function is zero if we use the optimal policy $u=u_{opt}(d)$. The loss has the advantage of providing a better “absolute scale” on which to judge whether a given set of controlled variables c is “good enough”, and thus is self – optimizing.

4.3.2 Open Loop Implementation:

Let us first consider an open-loop implementation where we attempt to keep u constant at the value u_S . With this implementation the operation may be non-optimal (with a positive loss) due to the following reasons

1. The value of u_S is different from the optimal value $u_{opt}(d)$.
2. The actual value of u is different from u_S (due to an implementation error caused by imperfect control).

This can be seen more clearly if we write the actual input as:

$$u = u_S + e_u \quad (4.5)$$

Where e_u is the implementation error for u . In process control, u is often a flow rate, and it is difficult in practice to obtain exactly the desired value u_S , so e_u may be large.

Introducing the optimization error:

$$e_{u,opt}(d) = u_S - u_{opt}(d) \quad (4.6)$$

Then the difference between the actual and optimal input, which causes a positive loss, can be written:

$$u - u_{opt}(d) = u_S - u_{opt}(d) + e_u \quad (4.7)$$

It is the sum of the optimization error and the control error. In summary, the open-loop policy is often poor; both because the optimal input value often depends strongly on the disturbance (so $e_{u,opt}$ is large), and because we are not able to implement u accurately (so e_u is large).

4.3.3 Closed Loop Implementation

In theory, the truly optimal solution would be to use some “optimizing controller” which uses the measurements information (feedback) to correct the model and estimate the disturbance d , and based on this computes a new optimal value $u_{op}(d)$. The main problem with this approach is the modeling effort, and the lack of theoretical tools to ensure robustness (insensitivity to uncertainty).

As mentioned, in practice, a simpler closed-loop implementation is preferred if it yields acceptable operation (loss). This approach uses directly the measurements c_m of the selected controlled variables and adjusts u in an inner feedback loop to achieve $c_m \gg c_S$, where in most cases $c_S = c_{op}(d_0)$, i.e. c_S comes from solving the nominal optimization problem. The idea is that by keeping $c_m \gg c_S$ we achieve an operation where the deviation $u - u_{op}(d)$ is smaller than for the open-loop policy (in the open-loop policy we keep u constant, but this is not optimal in the face of disturbances). This may happen because $c_{op}(d)$ is relatively insensitive to d and/ or because c may more accurately controlled.

We here rewrite the problem with the variables c as independent variables rather than the original independent variables (inputs) u . However, note that we as a special case may choose $c=u$, or some of the elements in the vector c may be the original input variables. Thus, the open-loop implementation is included as a special case.

More generally, if there are many alternative sets of variables c which can be measured and controlled, which set should be used? If we let y_m represent all the candidate measured variables then we can write:

$$c = g(y_m, u) \quad (4.8)$$

Where the function g is free to select. An open loop policy is obtained with $g(y_m, u) = u$. Linearized in terms of deviation variables(4.8) becomes:

$$\Delta c = C_1 \Delta y_m + C_2 \Delta u \quad (4.9)$$

The issue is then to find the optimal choice for the matrices C_1 and C_2 , but under the restriction that the number of controlled variables (c 's) equals the number of independent inputs (u 's). If we use only feedback then $C_2=0$. If we do not allow “combined” controlled

variables, then the matrix $C = [C_1 C_2]$ is a selection matrix with only one nonzero element in each row.

To compare the alternative choices we may evaluate the objective function, or equivalently the loss function, for alternative values of the disturbance d and the implementation error e_c . The optimal choice for controlled variables c (i.e. optimal choice of the matrix C) is then the one that minimizes some average value of the loss:

$$L(u, d) = L(f^{-1}(c_S + e, d), d) \quad (4.10)$$

For the expected set of disturbances $d \in D$, and expected set of implementation (control) errors $e \in E$. In the simplest case we select the setpoints as $c_S = c_{opt}(d_0)$, but the value of c_S may also be the subject to an optimization.

The difference between the actual and optimal outputs, which causes a positive loss, can be written:

$$c - c_{opt}(d) = c_S + e - c_{opt}(d) = e_{opt}(d) + e \quad (4.11)$$

It is the sum of the optimization error $e_{opt}(d) = c_S - c_{opt}(d)$ and the control error e . As already mentioned, if there were no uncertainty (i.e. $d=d_0$ and $e_c=0$), then it would make no difference which variable c that were chosen.

Figure 4.1 illustrates an example where we may reduce the loss due to the disturbances by keeping the variable c constant instead of the input u . However, some loss must be expected due to the error associated with each approach, and for small disturbances the worst case error contribution will usually dominate the loss.

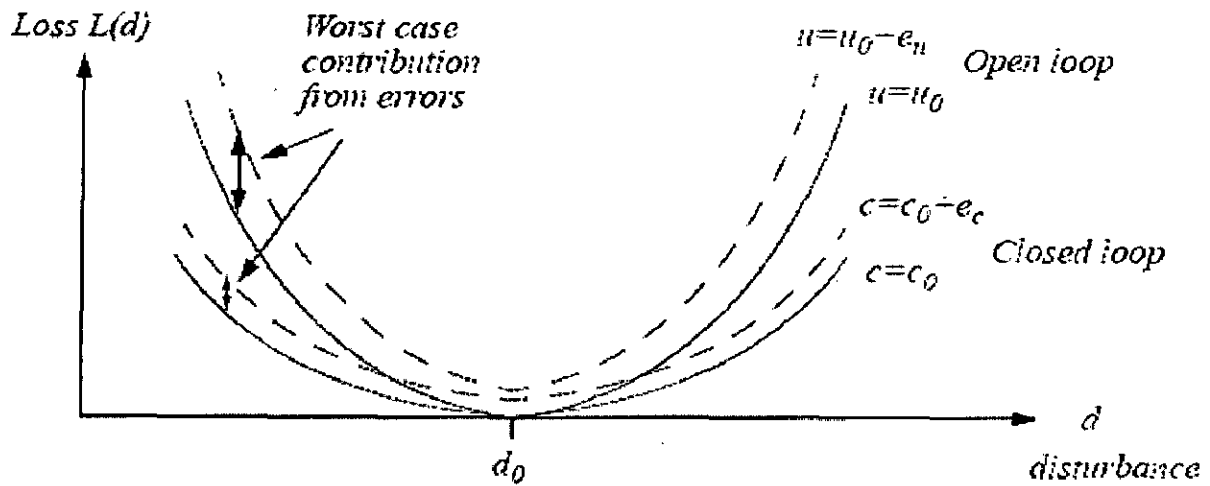


Figure 4.2: Loss as a function of disturbances for open loop and closed loop operation. The plot also illustrates the worst case contribution from the uncertainties and errors associated with each approach (dashed).

4.3.4 A Procedure For output Selection:

We are now in a position to formulate a procedure for selecting controlled outputs c . Preferably, one should find several candidate sets of candidate outputs, which could be further analyzed to see if they are adequate with respect to other criteria that may be relevant, such that the input-output controllability (including the presence of right half-plane zeros).

1. Define the optimal operation problem (including specifying the cost function J to be minimized).
2. Solve the optimization problem at a given nominal operating point. That is, find $u_{opt}(d_0)$ by solving the nominal optimization problem

$$\min_u J(u, d_0) \tag{4.12}$$

3. This yields a table with the nominal optimal values of all variables, $C_{opt}(d_0)$

4. Define the uncertainty for:

- **the optimization:** Define the magnitude or set of unknown disturbances ($d \in D$) (including any changes that occur between each reoptimization). Treat also errors in the data and model for the optimizer as disturbances.
- **each candidate output variable (y):** Define the magnitude or set of control error ($e \in E$) (e.g. due to measurement error)

5. Repeat for each *candidate set* of N_u output variables (y 's)

- Evaluate the cost function $J(c,d)$ with fixed setpoints

$$c = c_s + e \quad (4.13)$$

- Compute the “mean” cost, J_{mean} (or equivalently, the loss L)

6. Select as the controlled outputs the candidate set with the lowest “mean” cost (or retain all the sets with an acceptable loss for further screening).

4.4 Local Taylor Series Analysis

In this section we study the problem of selecting controlled outputs by expanding the cost function around a nominal optimal unconstrained operating point. To this end, we assume that the cost function J is smooth, or more precisely twice differ-entiable, at the operating point we are considering.

We assume that the nominal disturbance is d_0 and that the nominal operating point is optimal, i.e.

$$u_o = u_{opt}(d_o) \quad \text{and} \quad c_o = c_{opt}(d_o) \quad (4.14)$$

So that we have $J(u_o, d_o) = J_{opt}$. We next consider a disturbance and input change so that the new disturbance is:

$$d = d_o \Delta d \quad (4.15)$$

And the new input is:

$$u = u_o + \Delta u \quad (4.16)$$

Where Δu is the input change. The input u will generally be different from the optimal input, $u_{opt}(d)$, and we define the deviation from the optimal value as:

$$\Delta u' = u - u_{opt}(d) \quad (4.17)$$

Δu is not the same as $\Delta u'$, and more precisely $\Delta u = u - u_{opt}(d)$. In order to track the optimum we require $\Delta u' = 0$, which implies $\Delta u = u_{opt}(d) - u_{opt}(d_o)$.

4.4.1 Expansion of the Cost Function

A second order Taylor expansion of the cost function can be written compactly on matrix form as :

$$J(u, d) = J(u_o, d_o) + \begin{bmatrix} J_u^T & J_d^T \end{bmatrix} \begin{bmatrix} \Delta u \\ \Delta d \end{bmatrix} + \frac{1}{2} \begin{bmatrix} \Delta u \\ \Delta d \end{bmatrix}^T H \begin{bmatrix} \Delta u \\ \Delta d \end{bmatrix} + O^3 \quad (4.18)$$

Where H is the Hessian matrix of J with respect to $\begin{bmatrix} \Delta u \\ \Delta d \end{bmatrix}$; $H \begin{bmatrix} J_{uu} & J_{ud} \\ J_{du} & J_{dd} \end{bmatrix}$

All the derivatives are evaluated at the optimal nominal operating point (with $d = d_o$ and $u = u_o = u_{opt}(d_o)$), as indicated by using the subscript o . we have:

$$J_u = \left(\frac{\partial J}{\partial u} \right)_o = \left[\left(\frac{\partial J}{\partial u_1} \right)_o \quad \left(\frac{\partial J}{\partial u_2} \right)_o \quad \dots \quad \left(\frac{\partial J}{\partial u_n} \right)_o \right]^T = 0$$

$$J_d = \left(\frac{\partial J}{\partial d} \right)_o = \left[\left(\frac{\partial J}{\partial d_1} \right)_o \quad \left(\frac{\partial J}{\partial d_2} \right)_o \quad \dots \quad \left(\frac{\partial J}{\partial d_m} \right)_o \right]^T = 0$$

$$J_{uu} = \left(\frac{\partial^2 J}{\partial u^2} \right)_o = \begin{bmatrix} \left(\frac{\partial^2 J}{\partial u_1^2} \right)_o & \left(\frac{\partial^2 J}{\partial u_1 \partial u_2} \right)_o & \dots \\ \left(\frac{\partial^2 J}{\partial u_2 \partial u_1} \right)_o & \left(\frac{\partial^2 J}{\partial u_2^2} \right)_o & \dots \end{bmatrix} \quad (4.19)$$

$$J_{dd} = \left(\frac{\partial^2 J}{\partial d^2} \right)_o$$

$$J_{ud} = \left(\frac{\partial^2 J}{\partial u \partial d} \right)_o = \begin{bmatrix} \left(\frac{\partial^2 J}{\partial u_1 \partial d_1} \right)_o & \left(\frac{\partial^2 J}{\partial u_1 \partial d_2} \right)_o & \dots \\ \left(\frac{\partial^2 J}{\partial u_2 \partial d_1} \right)_o & \left(\frac{\partial^2 J}{\partial u_2 \partial d_2} \right)_o & \dots \end{bmatrix} = J_{du}^T$$

$J=0$ because the Jacobian with respect to the independent variables must be zero at the optimum when it is unconstrained. The Hessian matrix is always symmetric, so J_{uu} and J_{dd} are symmetric. Since the expansion is performed at the point where J has a minimum, we have that $Du^T J_{uu} Du$ is positive for any nonzero vector $D u$, i.e. J_{uu} is positive definite, $J_{uu} > 0$ (if the minimum is a saddle then $Du^T J_{uu} Du$ is zero in some direction and J_{uu} is positive semidefinite, $J_{uu} > 0$). Equation (4.18) written in separate terms in u and d gives:

$$J(u, d) = J(u_o, d_o) + J_u^T (u - u_o) + J_d^T (d - d_o) + \frac{1}{2} (u - u_o)^T J_{uu} (u - u_o) + \frac{1}{2} (d - d_o)^T J_{dd} (d - d_o) + (d - d_o)^T J_{du} (u - u_o) + O^3 \quad (4.20)$$

4.4.2 The Optimal input

The nominal operating point (u_0, d_0) is assumed to be optimal so we have $u_0 = u_{opt}(d_0)$, and as noted the Jacobian must be zero ($J_u = 0$). Next, consider a disturbance and a corresponding optimal input change so that the new operating point is (u, d) and the new Jacobian is:

$$J'_u = \frac{\partial}{\partial u} J(u, d) \quad (4.21)$$

A first order expansion of the Jacobian at the nominal point gives:

$$J'_u = J_u + J_{uu}(u - u_o) + J_{ud}^T(d - d_o) + \mathcal{O}^2 \quad (4.22)$$

We assume that change the input so that the new operating point is also optimal, i.e. $u = u_{opt}(d)$. then we must have that the Jacobian is zero, i.e. $J'_u = 0$, and we get:

$$0 = J_{uu}(u_{opt}(d) - u_{opt}(d_o)) + J_{ud}^T(d - d_o) \quad (4.23)$$

Solving with respect to the input we find that a first order accurate approximation of optimal input when there is a disturbance change is:

$$u_{opt}(d) = u_o - J_{uu}^{-1} J_{ud}^T(d - d_o) \quad (4.24)$$

Thus $\Delta u_{opt} = u_{opt}(d) - u_o$ the optimal control action which will track a moving optimum as illustrated in Figure 4.2:

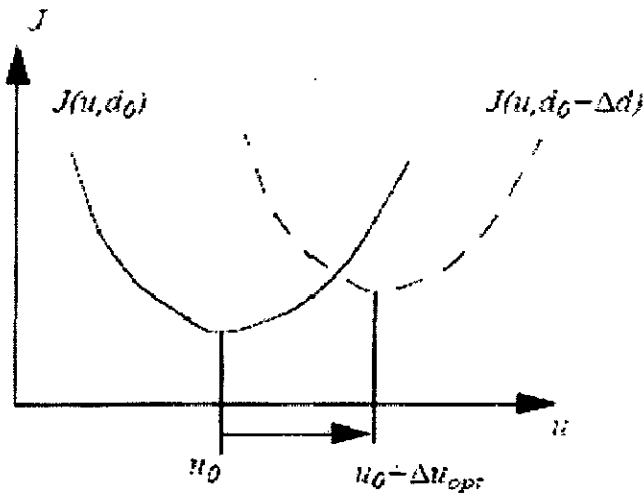


Figure 4.3: Optimal Control move

4.4.3 Expansion of the Loss Function

Let us now consider the loss function:

$$L(u, d) = J(u, d) - J(u_{opt}(d), d) \quad (4.25)$$

By applying the Taylor series expression in equation(4.20) and combining it with the loss function(4.24) we obtain the following interesting expression for the loss :

$$L(u, d) = \frac{1}{2} (u - u_{opt}(d))^T J_{uu}(u - u_{opt}(d)) = \Delta u'^T J_{uu} \Delta u' \quad (4.26)$$

Where $\Delta u' = u - u_{opt}(d)$. This tells that the loss is a function of the deviation ($\Delta u'$) from the optimal input which also intuitively is reasonable. Here the Hessian J_{uu} is evaluated in the nominal optimal point (u_0, d_0) . We might consider J_{uu}' evaluated at the current optimal point $(u_{opt}(d), d)$. However this does not matter as long as we only consider Taylor series expansion to the second order. This can be seen by expressing J_{uu}' in terms of J_{uu} . We have $J_{u'} = 0$ and

$$J_{uu}' = J_{uu} + J_{uud}^T(d - d_0) + J_{uuu}^T(u_{opt}(d) - u_{opt}(d_0)) \quad (4.27)$$

When we replace J_{uu} with J_{uu}' in (4.26) and remove the third order terms, we will get exactly the same expression. The impact from the disturbance (d) is only through $u_{opt}(d)$. This tells us that if the disturbances are small, or the disturbance has a small effect on the optimal input, the loss will also be small if we have an acceptable nominal input. The curvature described by the Hessian J_{uu} determines the “flatness” of the loss function.

This Chapter discusses results and interpretations of the analysis of a Petlyuk distillation column. The minimum energy solution for 3-product Petlyuk arrangement has been analyzed. The V_{min} -diagram gives a simple graphical interpretation of the whole operating space for 3-product distillation column. A key issue is that the feasible operating space is only dependent of two degree of freedom and the D-V plane spans this space completely. The distribution of feed components and corresponding minimum energy requirement is easily found by just having a glance at the diagram. The characteristic peaks and knots are easily computed by equation of Underwood and represent minimum energy operation for sharp split between all possible pairs of key components. The solutions can be very easily visualized in the V_{min} -diagram for the feed and given by the following rule:

“The minimum total vapor flow requirement in a Petlyuk arrangement is the same as the required vapor flow for the most difficult split between two of the specified products if that separation was to be carried out in a single conventional two-product column”.

5.1 Model Validation:

A saturated feed of ternary mixture of Methanol (A), Isopropanol (B) and n-Propanol (C) have been considered. The relative volatilities are 4.2, 1.86 and 1.00 respectively, and the feed compositions are 0.3, 0.3 and 0.4 respectively.

The above example was solved by the proposed model and the values of $\Theta_A=2.74067$ and $\Theta_B=1.28512$ were obtain. The Figure 5.1 shows that minimum energy required separating the saturated feed of ternary mixture of Methanol, Isopropanol and n-Propanol. P_0 - P_{AC} - P_1 is the region where both Underwood's root Θ_A and Θ_B are active and the ternary mixture ABC was splitted into two regions AB and BC completely at the point P_{AC} . Then the mixtures AB and BC were separated into the pure product A, B and C at the points

P_{AB} and P_{BC} respectively. The values of vapor flow rates at the peaks (i.e. P_{AC} , P_{AB} and P_{BC}) are given in the Table 5.1.

Table 5.1 Vapor Flow Rates at the Peaks and Knots in the V_{min} – diagram for ternary mixture of Methanol, Isopropanol and n - Propanol (For Model Validation).

$\alpha[4.20, 1.86, 1.00]$ and $z[0.3, 0.3, 0.4]$					
$\Theta_A = 2.741$ $\Theta_B = 1.285$	P_O	P_{AB}	P_{BC}	P_{AC}	P_I
V_{Tmin}	0	0.8634	1.4029	0.6930	0
D	0	0.30	0.60	0.38	1

The minimum total vapor flow requirement in a Petlyuk arrangement to separate the given ternary mixture ABC was found to be 1.4029 times than feed flow rate. The results was compared with the solved example given in the book “Conceptual Design of Distillation Systems” by Doherty, M.F. and Malone, M.F. [6] to separate the same ternary mixture from conventional distillation column [6]. The minimum vapor required to separate the given mixture with conventional distillation column is 2.2095 times the feed flow rate. Hence 36.6% energy saving was achieved by using Petlyuk distillation column instead of conventional distillation column.

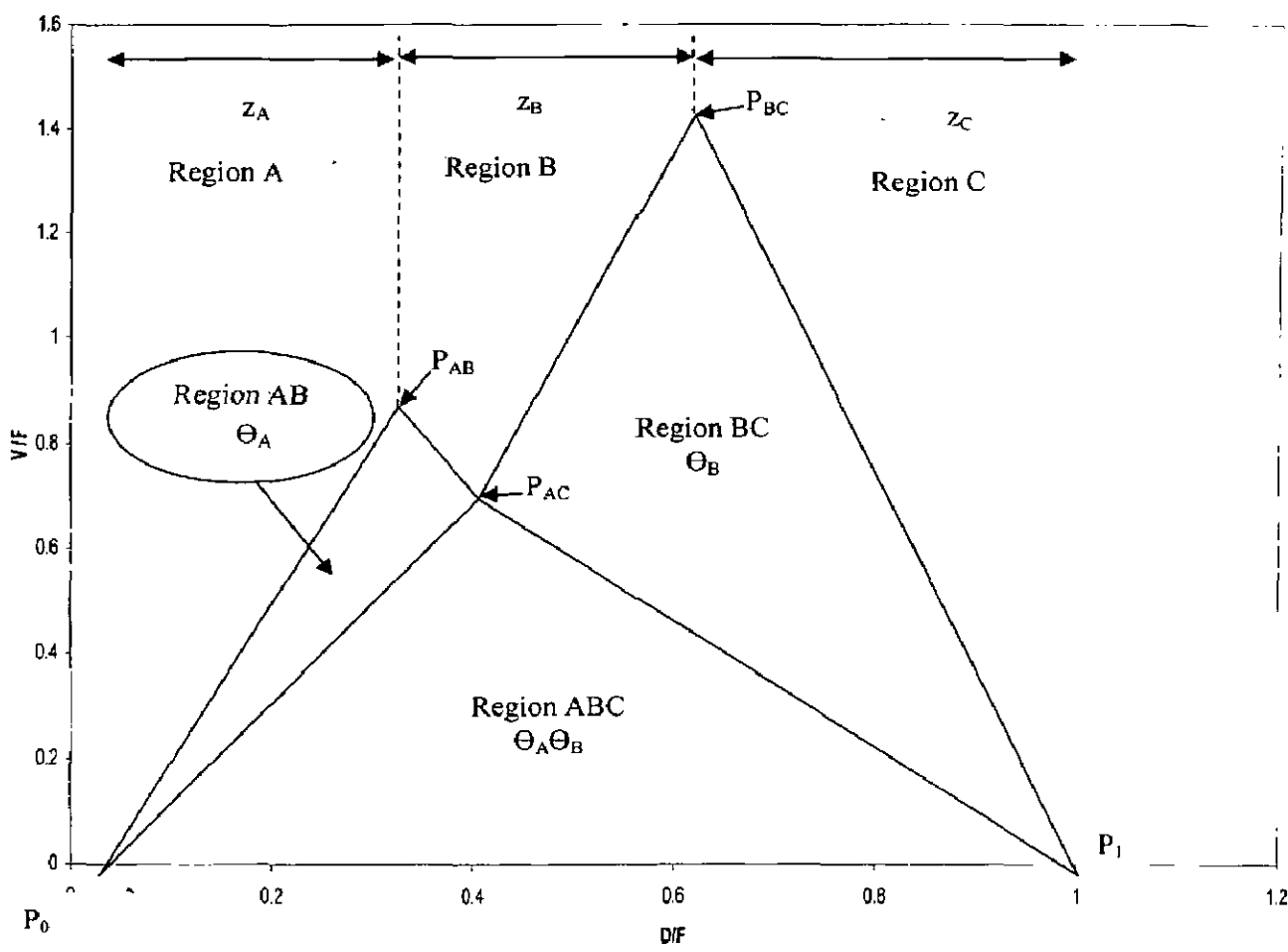


Figure 5.1: Vmin – Diagram for the ternary mixture of Methanol, Isopropanol and n-Propanol

5.1.1 Case study-I: Four Component Feed (ABCD)

A partly vapor feed ($q = 0.8$) of four component mixture ABCD was considered for case study. The relative volatilities were 14.00, 7.00 3.00 and 1.00 respectively, and the feed compositions were 0.25, 0.25, 0.25 and 0.25.

Table A.2 Vapor Flow rates at the Peaks and Knots in the V_{min} – diagram for Case Study (I): Four Product separation.

$\alpha[14, 7, 3, 1]$ and $z[0.25, 0.25, 0.25, 0.25]$								
	P_0	P_{AB}	P_{BC}	P_{CD}	P_{AC}	P_{BD}	P_{AD}	P_1
V_{Tmin}	0	.08975	0.9585	1.0248	0.6350	0.7311	0.5501	0.2
D	0	0.25	0.50	0.75	0.3663	0.5839	0.4490	1

The above problem solved by Underwood's Classical equation for minimum energy. Figure 5.2 shows that the minimum energy required to separate the partly vapor feed of 4-components ABCD. P_0 - P_{AD} - P_1 was the region where all three Underwood's root Θ_A , Θ_B and Θ_C were active and mixture ABCD splits into two regions ABC and BCD completely at the point P_{AD} . P_0 - P_{AC} - P_{AD} was the region where only Θ_A and Θ_B were active and the mixture ABC again splits into two regions AB and BC at point P_{AC} . Similarly, P_{AD} - P_{BD} - P_1 was the region where two roots Θ_B and Θ_C were active and mixture BCD splits into two regions BC and CD at point P_{BD} . Finally, the mixtures AB, BC and CD was separated into the pure product A, B, C and D at the points P_{AB} , P_{BC} and P_{CD} respectively. The vapor flow rates at the peaks (i.e. P_{AD} , P_{AC} , P_{BD} , P_{AB} , P_{BC} and P_{CD}) are shown in Figure 5.2 and vales are given in the Table 5.2. V_{min} required in Petlyuk distillation column was found to be 1.0248 times the feed flow rate.

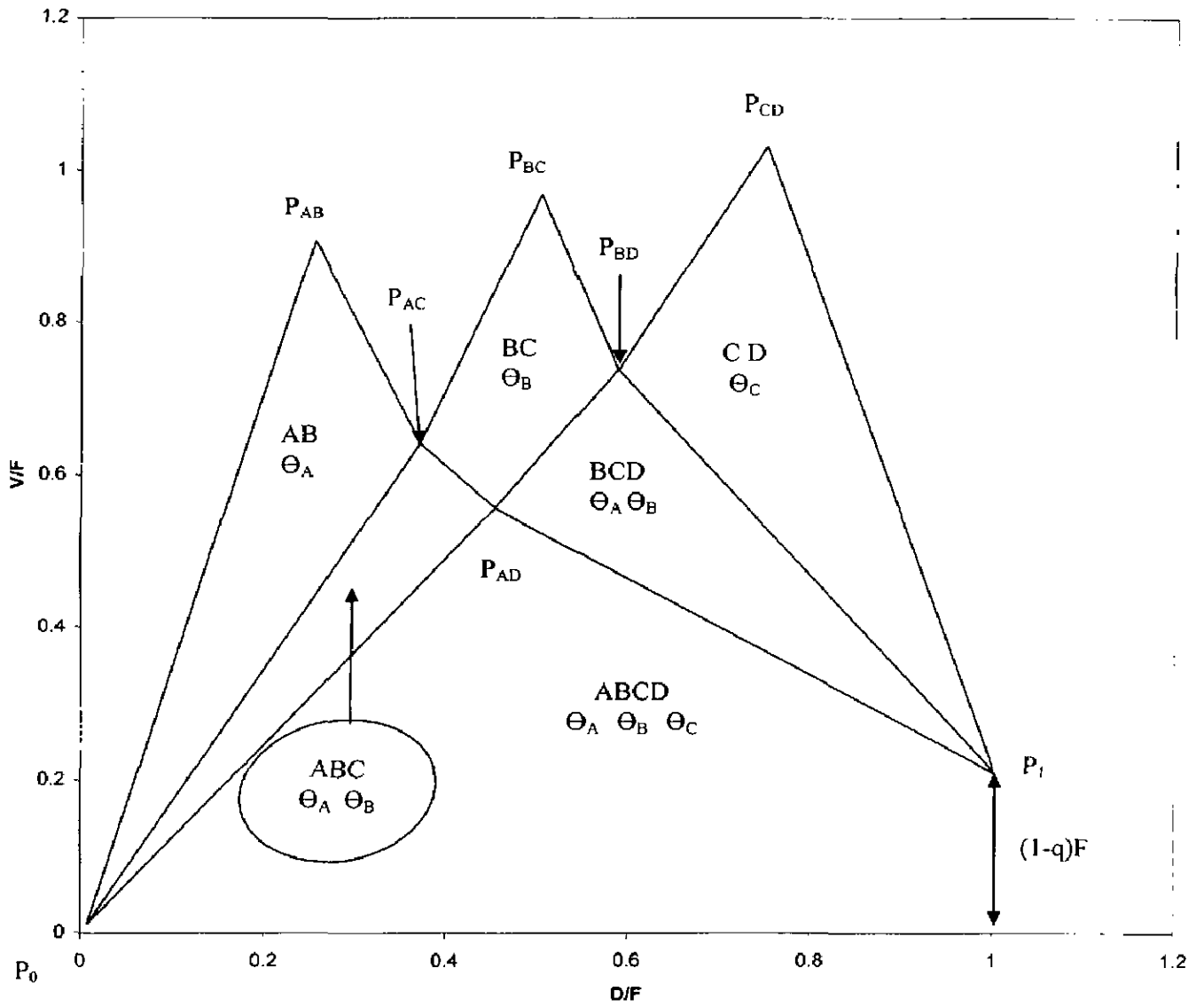


Figure 5.2: V_{min} - Diagram for the Case Study (I): Four Component Feed (ABCD)

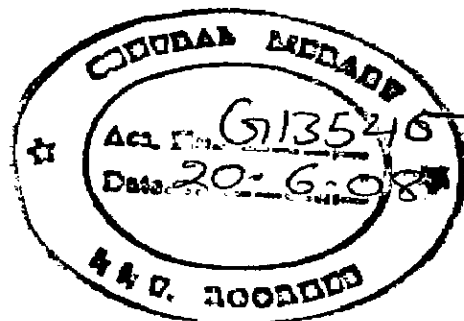
5.1.2 Case Study II: Ternary Feed (ABC)

A saturated feed of ternary mixture ABC was considered for case study. The relative volatilities were 4.00, 2.00 and 1.00 respectively, and the feed compositions were 0.333, 0.333 and 0.333.

Table 5.3 Vapor Flow rates at the Peaks and Knots in the V_{min} – diagram for Case Study (II)

$\alpha[4, 2, 1]$ and $z[0.333, 0.333, 0.333]$					
$\Theta_A = 2.756$ $\Theta_B = 1.243$	P_0	P_{AB}	P_{BC}	P_{AC}	P_1
V_{Tmin}	0	1.0707	1.3642	0.7767	0
D	0	0.333	0.667	0.444	1

The case-II solved by the proposed model and the values of $\Theta_A=2.756$ and $\Theta_B=1.243$ were obtained. The Figure 5.3 shows, minimum energy required to separate the saturated feed of ternary mixture ABC. P_0 - P_{AC} - P_1 was the region where both Underwood's root Θ_A and Θ_B were active and the ternary mixture ABC splits into two regions AB and BC completely at the point P_{AC} . Similarly, the mixtures AB and BC have been separated into the pure product A, B and C at the points P_{AB} and P_{BC} respectively. The vapor flow rates at the peaks (i.e. P_{AC} , P_{AB} and P_{BC}) are shown Figure 5.3 and values are given in the Table 5.3. V_{min} required in Petlyuk distillation column was found 1.3642 times the feed flow rate. The minimum vapor required to separate the given mixture with conventional distillation column is 2.03 times the feed flow rate [21]. Hence 32.8 % energy saving was achieved by using Petlyuk distillation column instead of conventional distillation column.



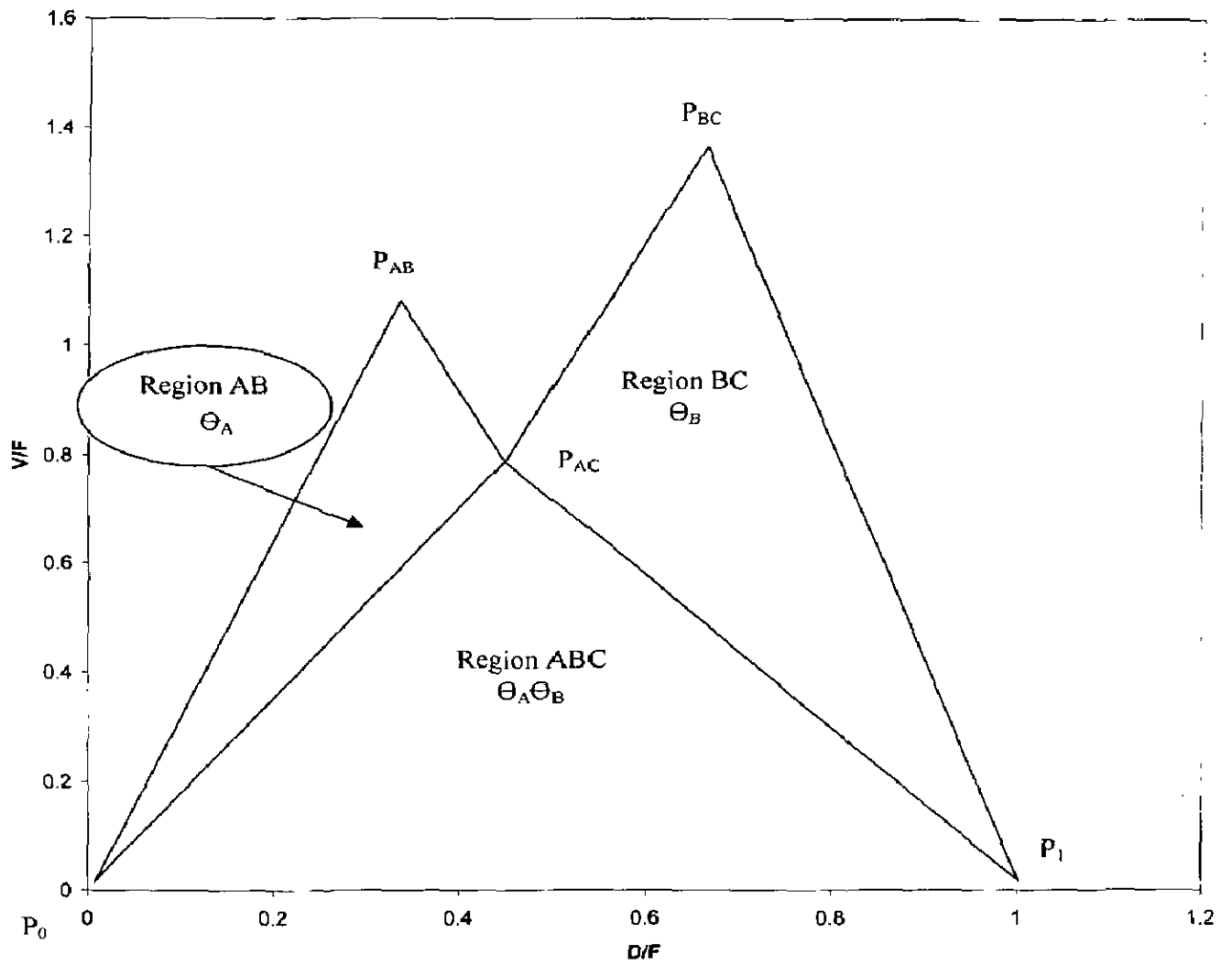


Figure 5.3: V_{min} - Diagram for the Case Study (II): Ternary Mixture (ABC)

5.2 Parameter Study

5.2.1 Variation in V_{min} at different Composition of more volatile

Component (Methanol)

Methanol is the most volatile and n- Propanol is the least volatile component in given ternary mixture. Hence, sharp B/C split is the more difficult split as compared to sharp A/B split. Composition change of methanol from 0.1 to 0.85 was done and 6 V_{min} – diagrams was obtained.

Table A.4 Vapor Flow rates at the Peaks and Knots in the V_{min} – diagram at the different composition of the saturated liquid feed.

$\alpha[4.20, 1.86, 1.00]$					
$z[z_A, z_B, z_C]$	P_0	P_{AB}	P_{BC}	P_{AC}	P_1
[0.1, 0.4, 0.5]	$\Theta_A=3.543$		$\Theta_B=1.325$		
V_{Tmin}	0	0.6393	1.5367	0.5203	0
D	0	0.10	0.50	0.2076	1
[0.2, 0.2, 0.6]	$\Theta_A=2.9272$		$\Theta_B=1.4738$		
V_{Tmin}	0	0.65996	1.2714	0.56646	0
D	0	0.20	0.40	0.2536	1
[0.3, 0.3, 0.4]	$\Theta_A=2.74067$		$\Theta_B=1.28512$		
V_{Tmin}	0	0.8634	1.4029	0.6931	0
D	0	0.30	0.60	0.3806	1
[0.4, 0.4, 0.2]	$\Theta_A=2.639$		$\Theta_B=1.128$		
V_{Tmin}	0	1.0762	1.5633	0.8198	0
D	0	0.4	0.8	0.5074	1
[0.7, 0.2, 0.1]	$\Theta_A=2.138$		$\Theta_B=1.071$		
V_{Tmin}	0	1.4255	1.4111	1.0660	0
D	0	0.70	0.90	0.7537	1
[0.85, 0.1, 0.05]	$\Theta_A=2.979$		$\Theta_B=1.037$		
V_{Tmin}	0	1.6074	1.3547	1.1891	0
D	0	0.85	0.95	0.8768	1

Figure 5.4-5.6 was analyzed and found that the minimum energy required for sharp A/B split was lower than the sharp B/C split. In figure 5.7 and Figure 5.8 the minimum energy required for sharp A/B split was greater than the sharp B/C split, hence it is infeasible to operate the Petlyuk distillation column in this higher energy consumption for sharp A/B split as compared to sharp B/C. From the point of view of energy saving, it is cleared from Figure 5.9 that we will operate Petlyuk distillation column less than 0.69 composition of Methanol.

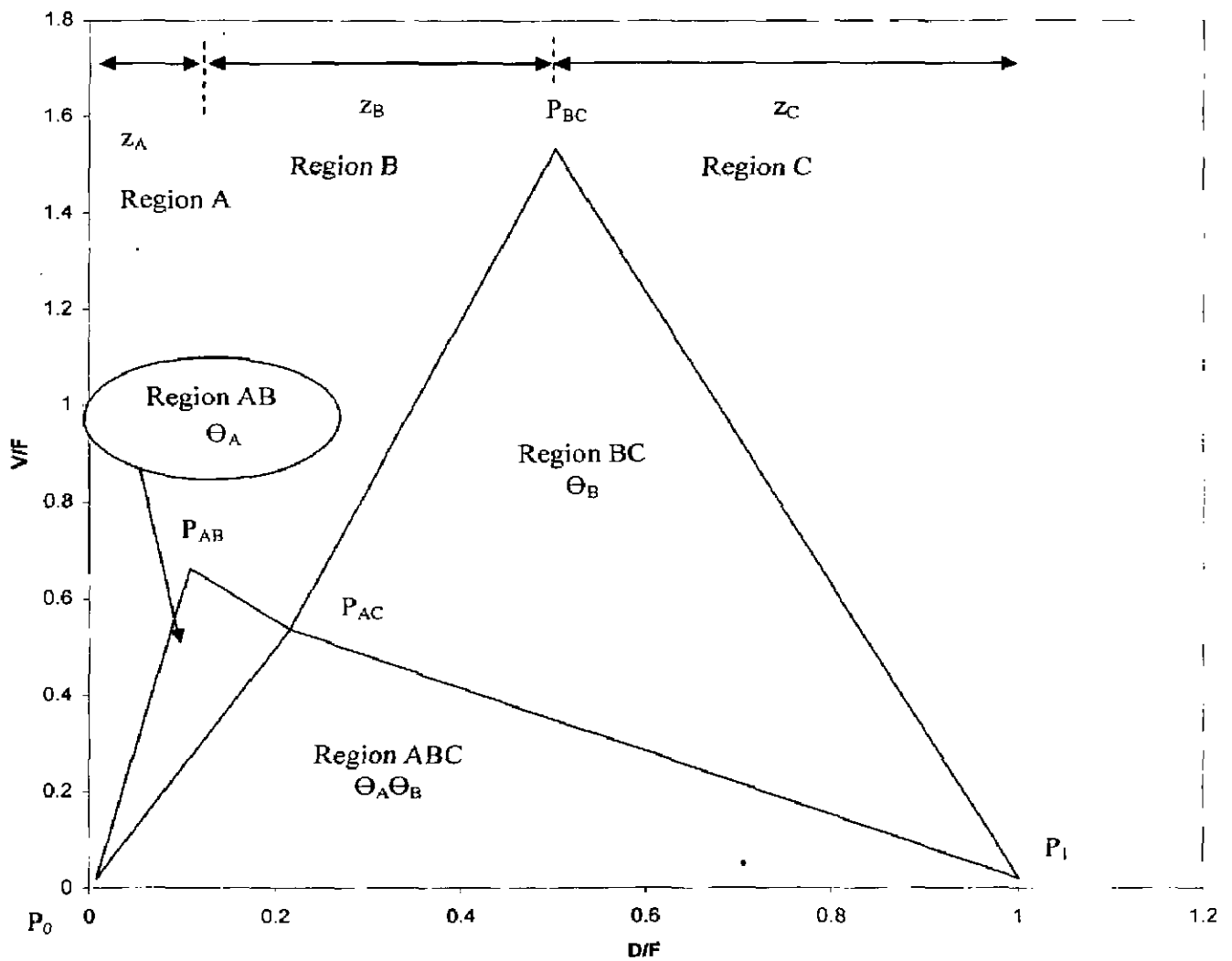


Figure 5.4: V_{min} - Diagram for the ternary mixture of Methanol, Isopropanol and n-Propanol at the feed composition of [0.1, 0.4, 0.5]

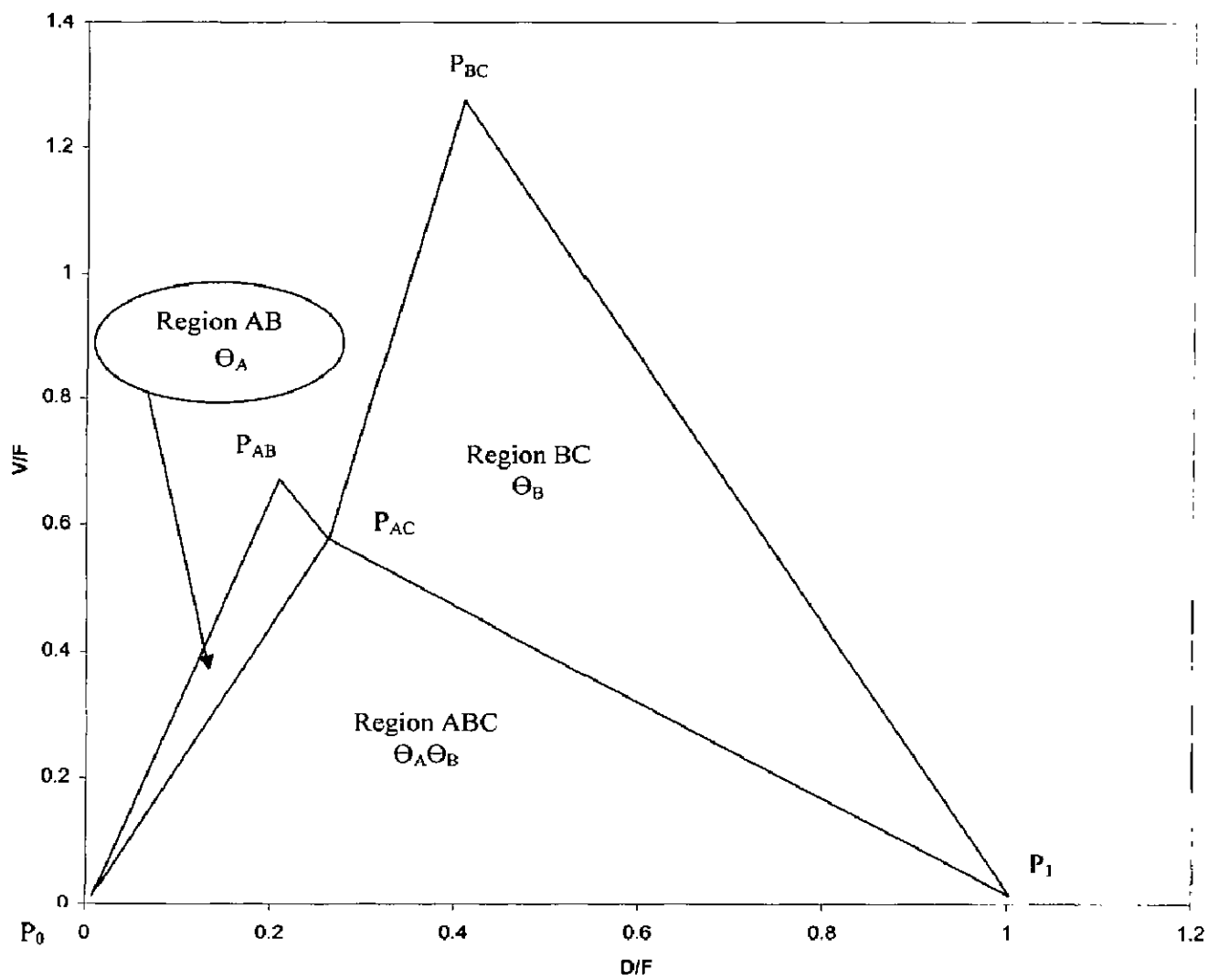


Figure 5.5: Vmin – Diagram for the ternary mixture of Methanol, Isopropanol and n- Propanol at the feed composition of [0.2, 0.2, 0.6]

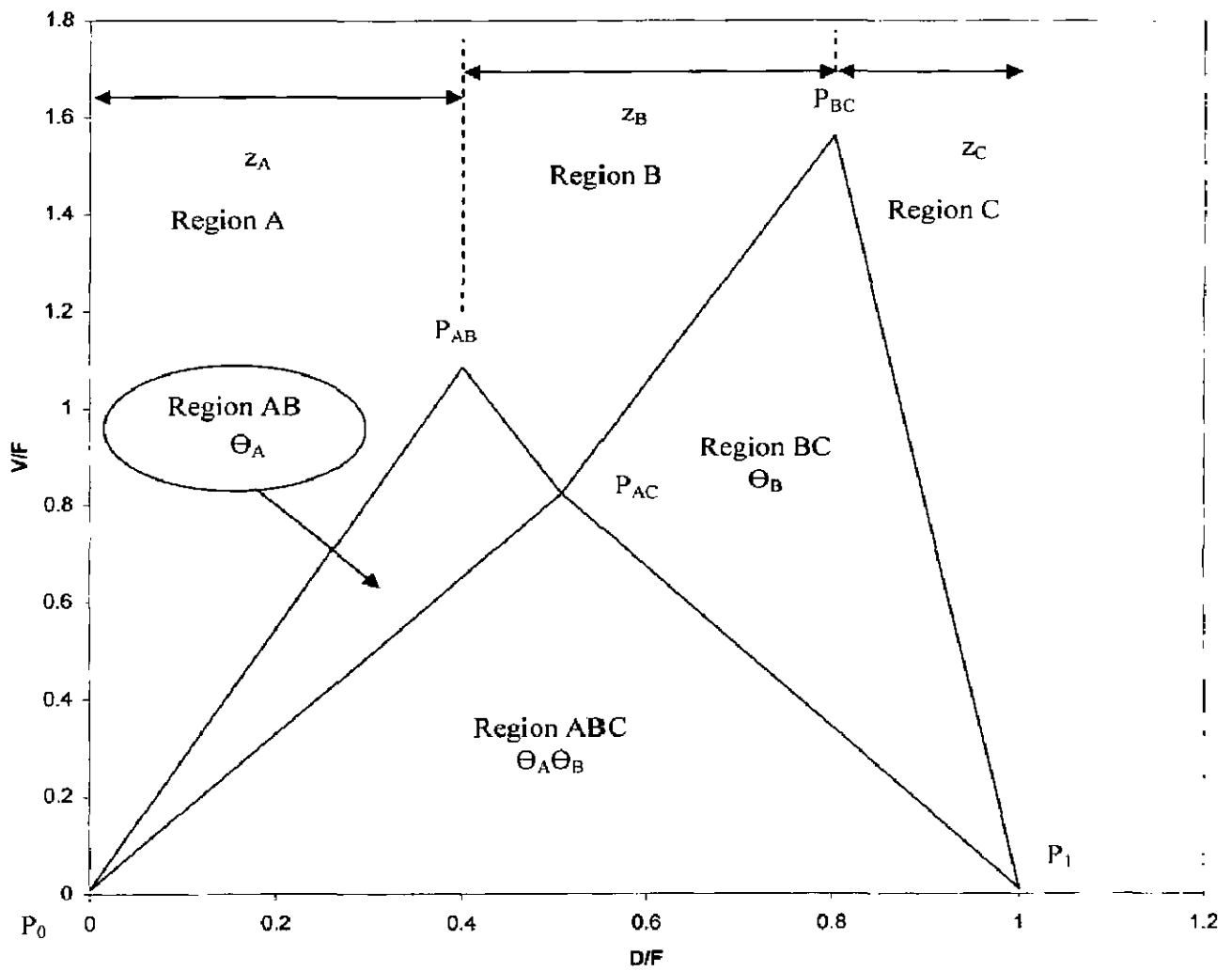


Figure 5.6: V_{min} – Diagram for the ternary mixture of Methanol, Isopropanol and n- Propanol at the feed composition of [0.4, 0.4, 0.2]

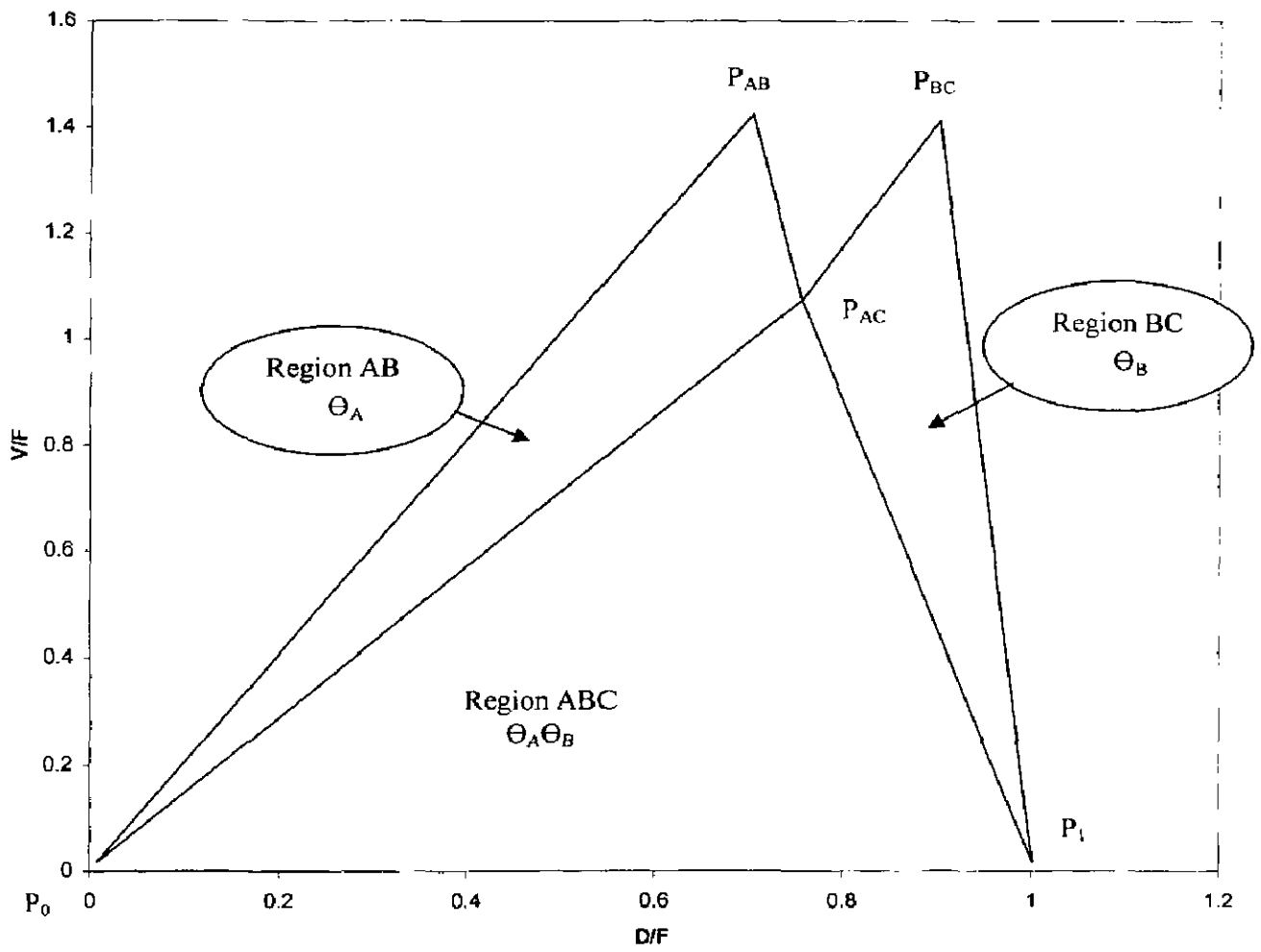


Figure 5.7: V_{min} – Diagram for the ternary mixture of Methanol, Isopropanol and n- Propanol at the feed composition of [0.7, 0.2, 0.1]

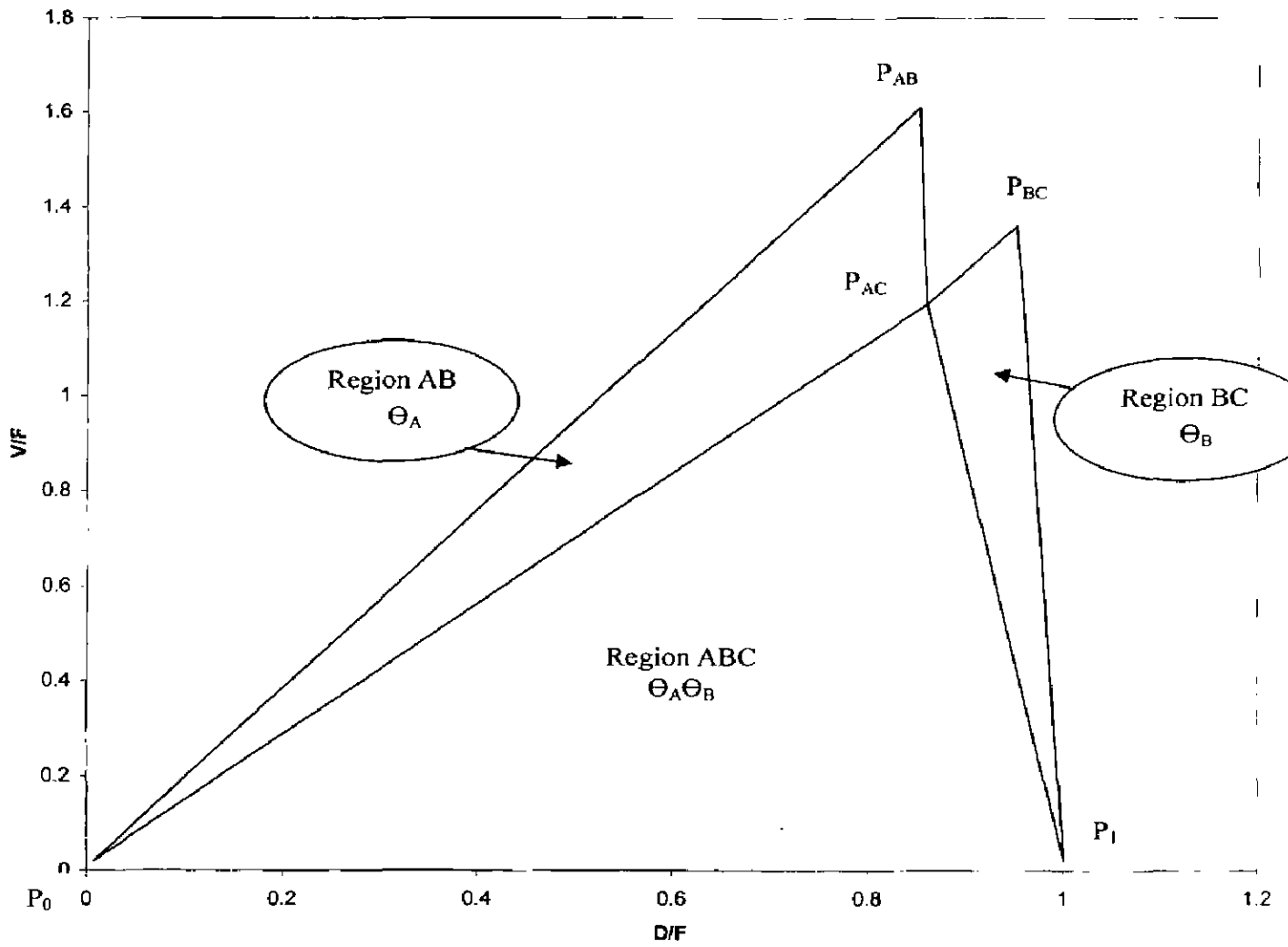


Figure 5.8: V_{min} – Diagram for the ternary mixture of Methanol, Isopropanol and n- Propanol at the feed composition of [0.85, 0.1, 0.05]

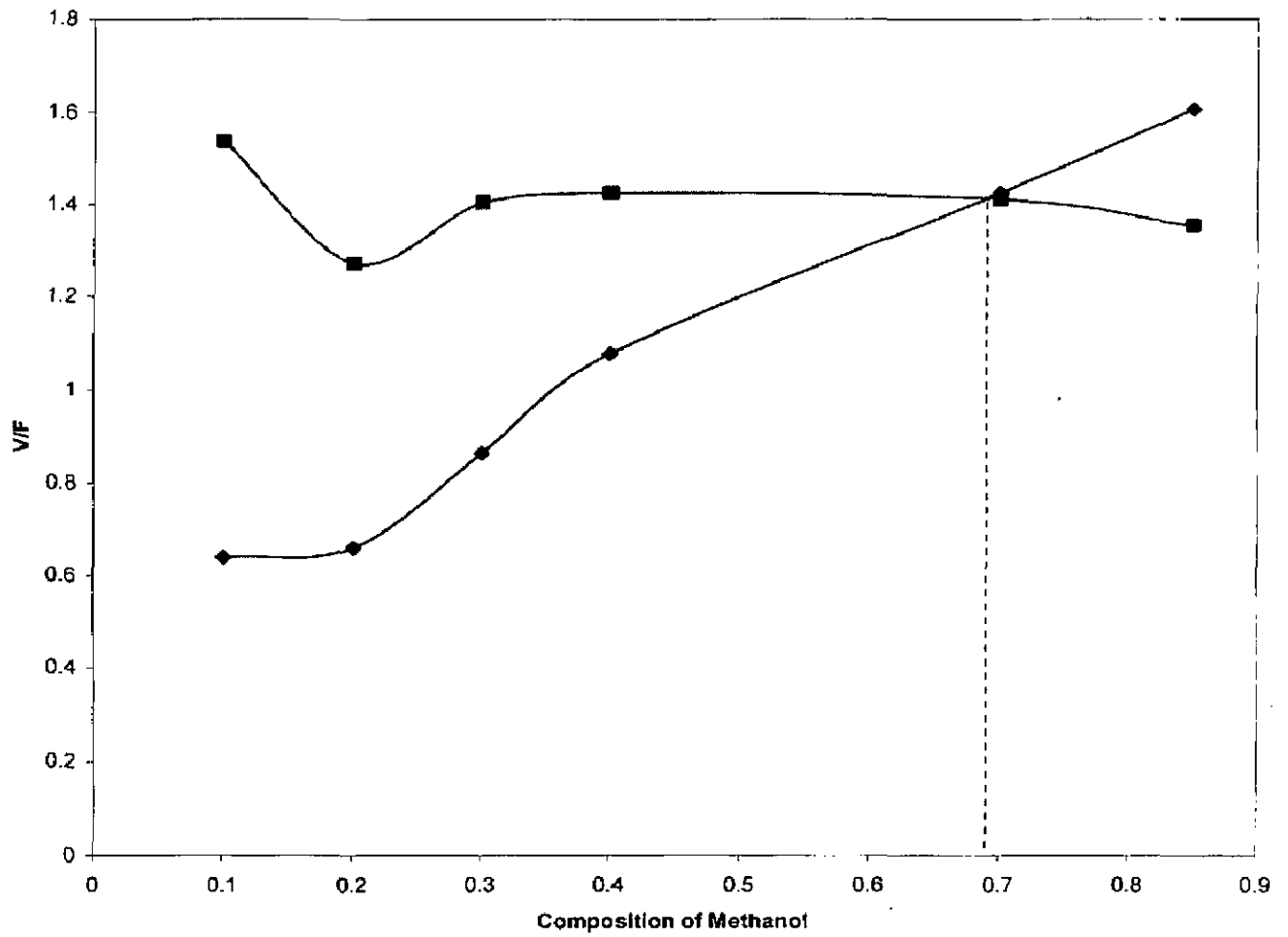


Figure 5.9 Comparison of minimum vapor flow requirement in Sharp A/B and B/C with respect to Composition of more Volatile Component (Methanol).

5.2.2 Variation in V_{\min} by Changing Feed Conditions

All five feed conditions were analyzed at the same composition of ternary mixture of Methanol, Isopropanol and n-Propanol. It was that when the value of liquid fraction (q) decreases in the feed then the minimum total vapor requirement in Petlyuk distillation column increases.

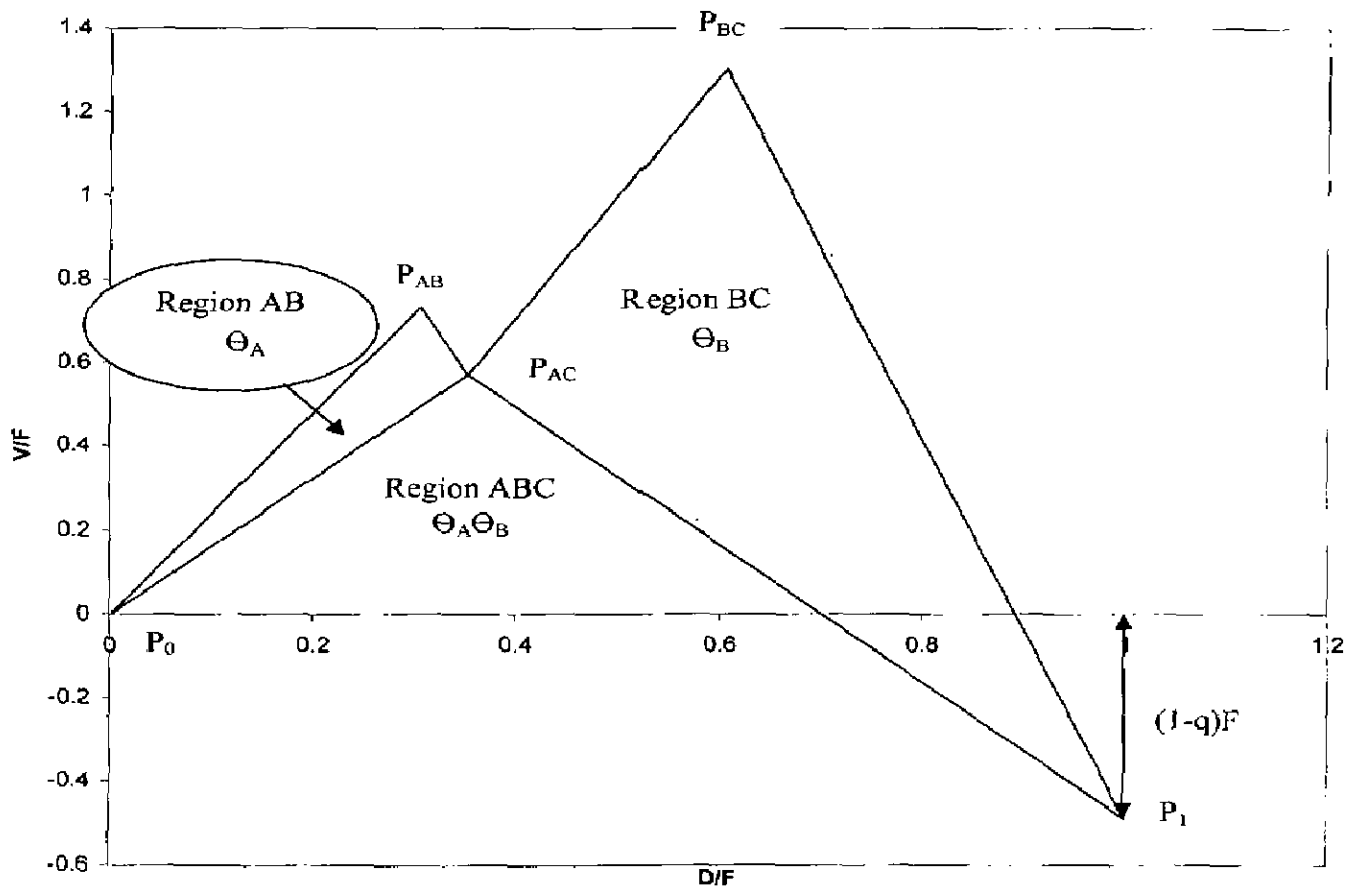


Figure 5.10: V_{\min} - Diagram for the Cold ternary mixture of Methanol, Isopropanol and n-Propanol at the feed composition of [0.3, 0.3, 0.4]

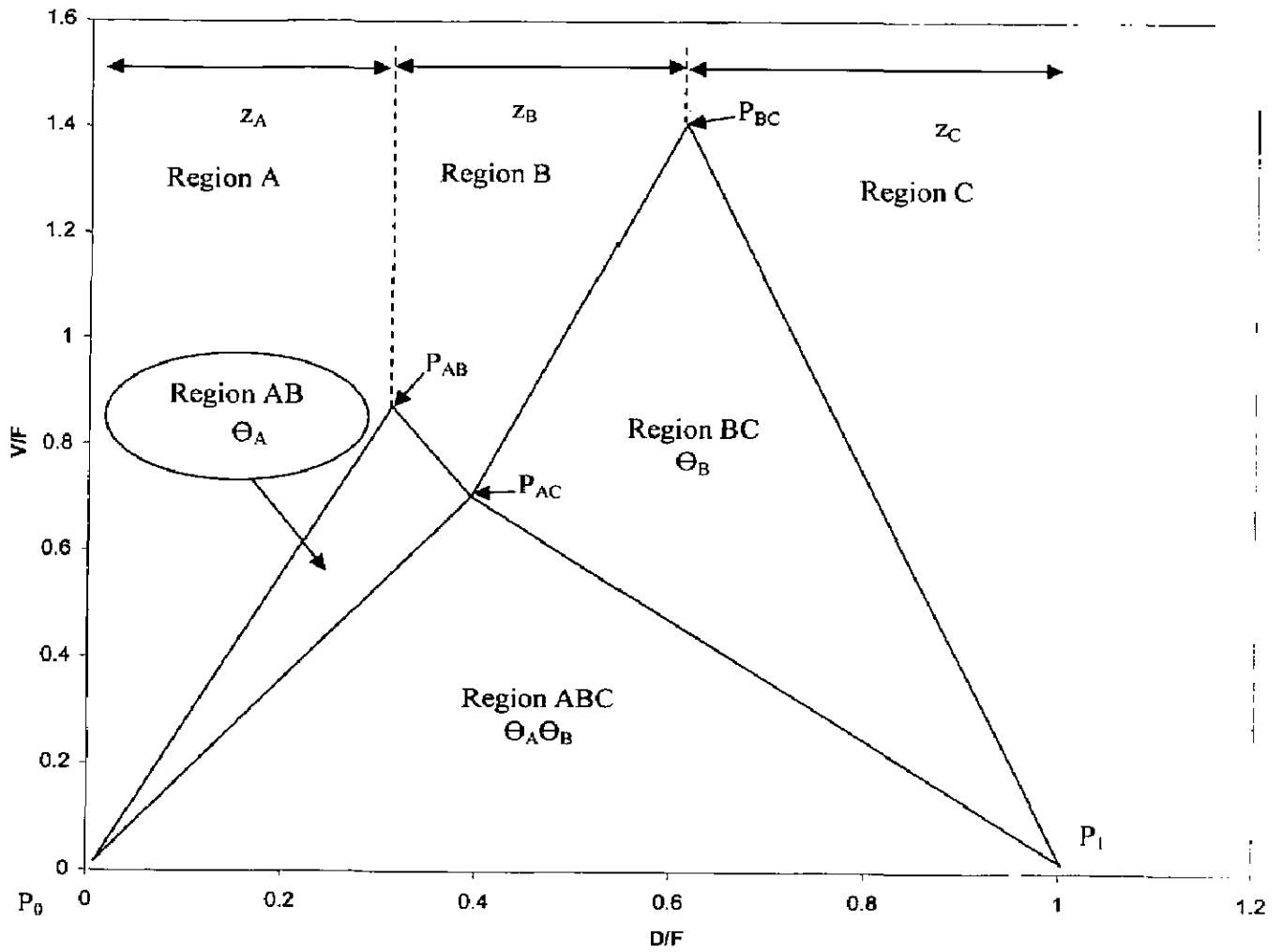


Figure 5.11: Vmin – Diagram for the Saturated Liquid mixture of Methanol, Isopropanol and n-Propanol at the feed composition of [0.3, 0.3, 0.4]

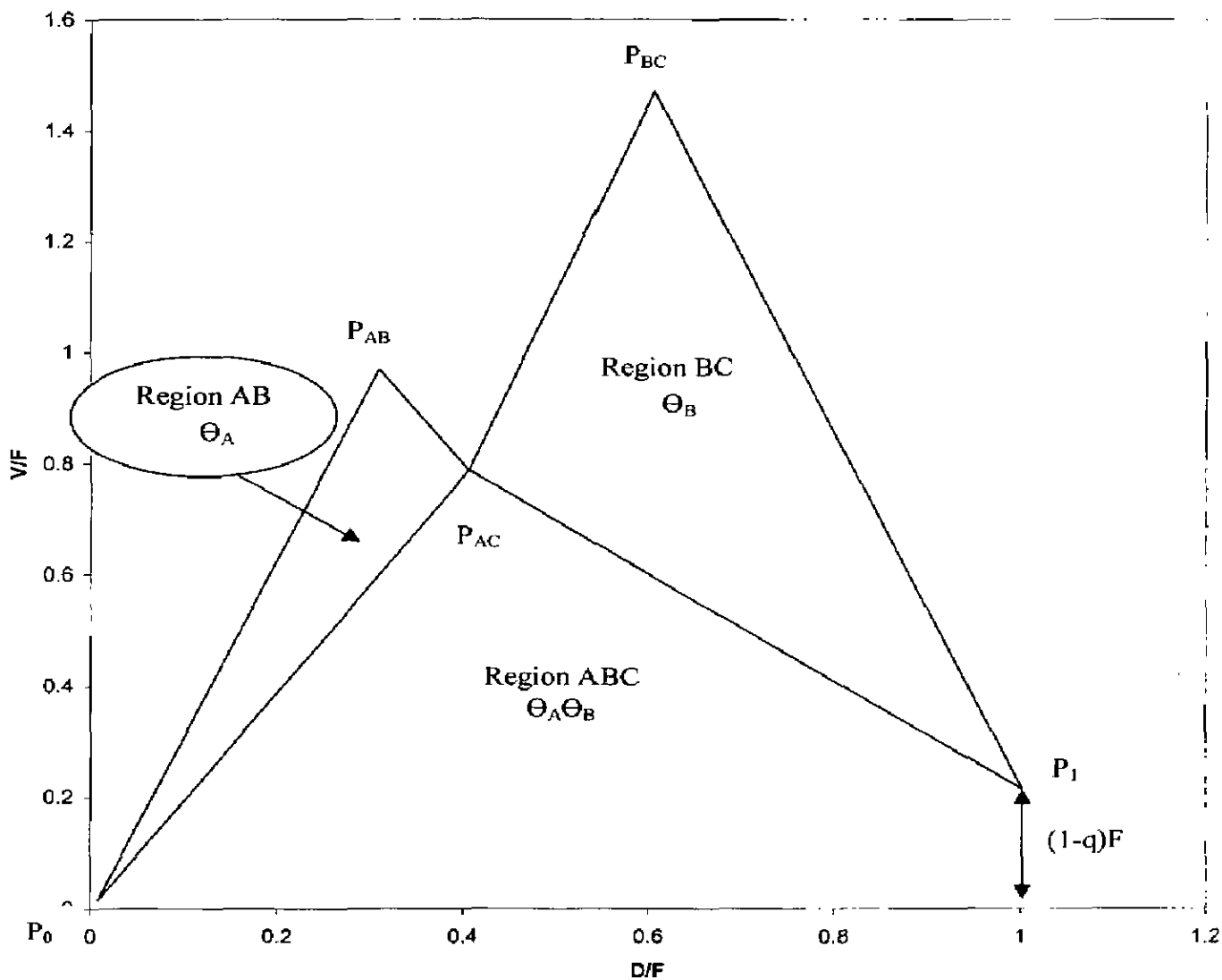


Figure 5.12: Vmin – Diagram for the Partly Vapor mixture of Methanol, Isopropanol and n- Propanol at the feed composition of [0.3, 0.3, 0.4]

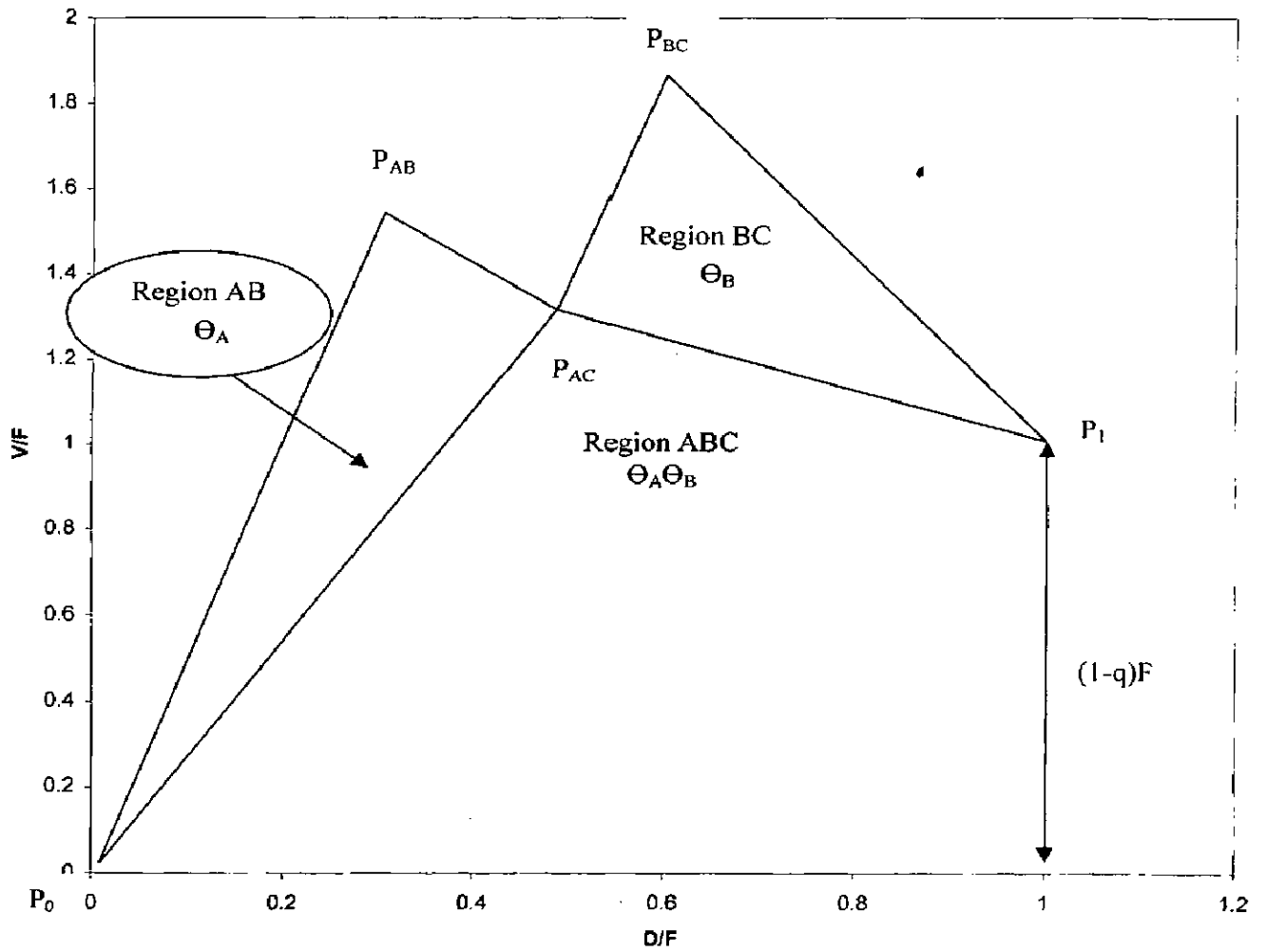


Figure 5.13: V_{min} – Diagram for the Saturated Vapor mixture of Methanol, Isopropanol and n-Propanol at the feed composition of [0.3, 0.3, 0.4]

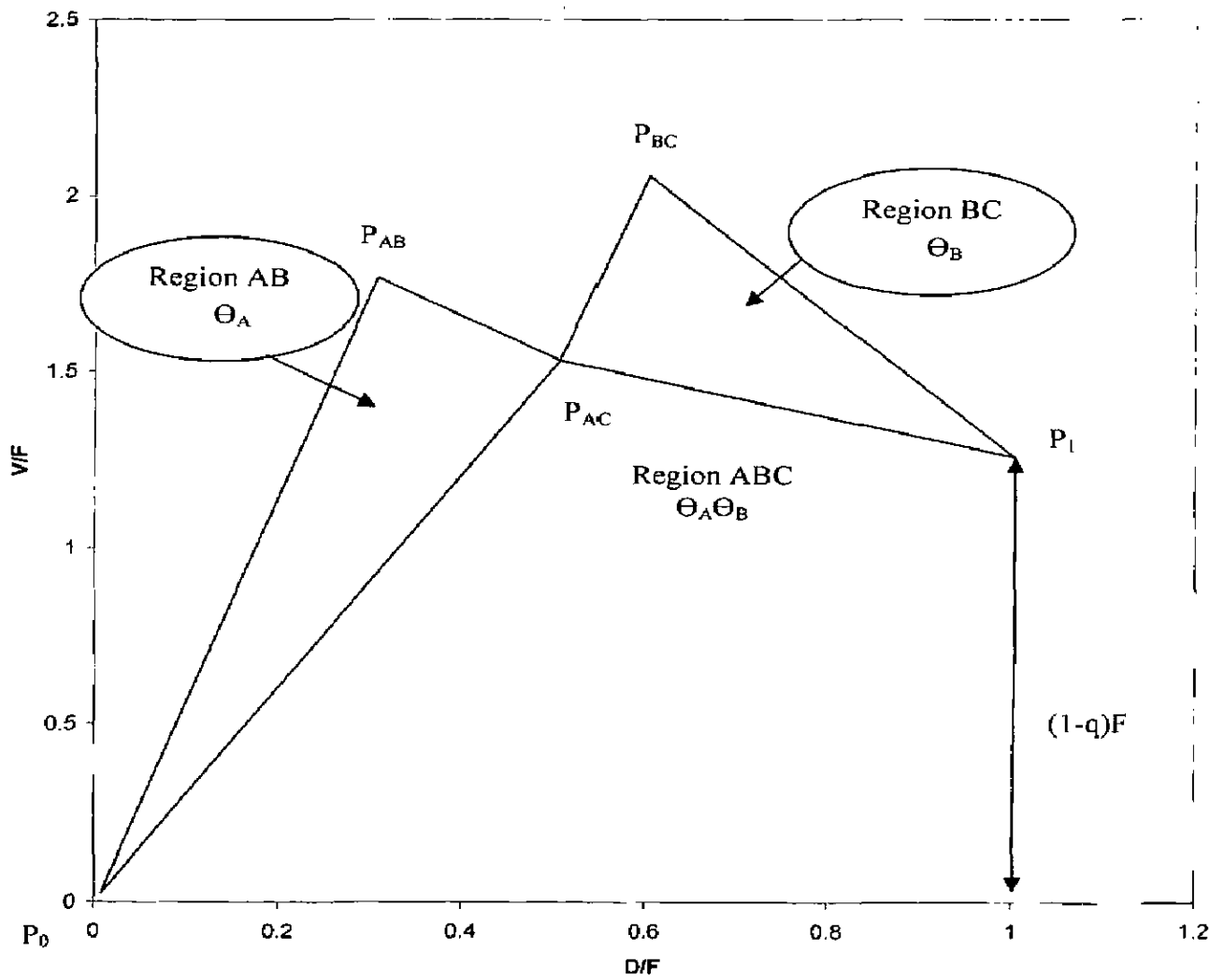


Figure 5.14: V_{min} - Diagram for the Superheated Vapor mixture of Methanol, Isopropanol and n- Propanol at the feed composition of [0.3, 0.3, 0.4]

CHAPTER 6

CONCLUSIONS AND RECOMMENDATIONS

6.1 Conclusions

The following major conclusions can be drawn from present work:

1. Underwood's Classical equations for minimum energy calculation has been derived for Petlyuk distillation column.
2. General analytic solution for minimum energy consumption in Petlyuk distillation column for multicomponent feed and any number of products have been derived.
3. The graphical tool (V_{min} -diagram) has been used to calculate the minimum energy requirement for the separation of ternary mixture of Methanol, Isopropanol and n- Propanol.
4. 36.6% energy saving has been achieved by using Petlyuk distillation column instead of conventional distillation column in the separation of ternary mixture of Methanol, Isopropanol and n- Propanol.
5. In the case study-I, the minimum vapor flow required to separate four component feed in Petlyuk distillation column has been found 1.0248 times the feed flow rate.
6. In case study-II, 32.8% energy saving has been achieved by using Petlyuk distillation column instead of conventional distillation column in the separation of ternary mixture.
7. Self optimizing control of Petlyuk distillation column using local Taylor series analysis by turning the optimization problem into a constant setpoint problem has been studied

6.2 Recommendations

6.2.1 Process Design

The main results presented in this dissertation are developed for ideal systems with constant relative volatility and constant molar flows. However, based on the new understanding, it is straightforward to develop engineering procedures for real azeotropic mixtures. Appendix B contains a simple example of how to use a standard simulator with standard two-product columns to find the characteristics of the minimum energy solution for a directly coupled arrangement.

We have assumed constant pressure. However, operation on different pressure levels is widely used in process design, and this issue calls for further studies also for directly integrated columns. This also applies for internal heat integration.

6.2.2 Control Structure Design

We have shown that it is very important to adjust the degrees of freedom on-line in order to track the minimum energy operating point. However, we have not carried out a detailed controllability study where we look at the combined requirements for composition control and minimum energy operation. The principle of self optimizing control for selection of controlled variables is promising, and the methods can be developed further. This is a general methodology and the coupled arrangements are just one application area. The idea is to achieve robust and simple control structures. This issue is of great importance both when we use simple and conventional controllers and advanced control with on line optimization.

6.2.3 Advanced Control

Model based predictive control has been applied with success on a series of process control applications, and we should also consider such methods for directly coupled arrangements. However, the most widespread solutions are designed for setpoint control only. The main advantages compared to conventional solutions are their ability to handle constraints and multivariable process interactions.

In a directly coupled distillation arrangement we need to operate close to minimum energy. Thus we really need to include a general profit criterion on-line in addition to setpoint deviation criteria. Typical solutions today involve steady state optimization at the highest level, which computes the setpoints for the lower levels.

Advanced control methods do not replace the need for good control structure design. Thus selfoptimizing control is well suited for control structure design also when we consider advanced model based methods. One consequence is that the models required for optimization may become simpler.

REFERENCES

1. Agrawal, R. and Fidkowski Z.T. (1998), "Are Thermally Coupled Distillation Columns Always Thermodynamically More Efficient for Ternary Distillations?" *Ind. Eng. Chem.Res*, **37**, 3444-3454.
2. Alstad, V., Skogestad, S. and Halvorsen, I. J. (2005), "Optimal Operation of a Petlyuk Distillation Column: Energy Savings by Over-fractionating", *Journal of Process Control*, **47**,201-212.
3. Annakou, O. and Mizsey, P. (1996), "Rigorous Comparative Study of Energy-Integrated Distillation Schemes", *Ind. Eng. Chem.Res*, **35**, 1877-1885.
4. Carlberg, N.A. and Westerberg, A.W. (1989a), "Temperature-Heat Diagrams for Complex columns. 3. Underwood's Method for the Petlyuk Configuration", *Ind. Eng. Chem. Res.* Vol. **28**, pp 1386-1397, 1989.
5. Carlberg, N.A. and Westerberg, A.W. (1989b), "Temperature-Heat Diagrams for Complex. Columns. 2. Underwood's Method for Side-strippers and Enrichers", *Ind. Eng. Chem. Res.* Vol. **28**, pp 1379-1386, 1989.
6. Doherty, M.F. and Malone, M.F. (2001), "Conceptual Design of Distillation Systems", McGraw Hill, International Edition 2001.
7. Dong, F., Lou, H., Goto, M. and Hirose, T. (1998), "A new PSA process as an extension of the Petlyuk distillation concept", *Separation and Purification technology*, **15**, 31-40.
8. Flores, O. A. Cardenas, J.C., Hernandez, S. and Rico-Ramirez, V. (2003) "Thermodynamic Analysis of Thermally Coupled Distillation (petlyuk distillation) Sequences", *Ind. Eng. Chem.Res*, **42**, 5940-5945.
9. Fidkowski, Z. and Krolikowski, L. (1986), "Thermally Coupled System of Distillation Columns: Optimization Procedure", *AIChE Journal*, Vol. **32**, No. 4, pp 537-546, 1986.
10. Fidkowski, Z. and Krolikowski, L. (1987), "Minimum Energy Requirements of Thermally Coupled Distillation Systems", *AIChE Journal*, Vol. **33**, No. 4, pp6 43-653, 1986.

11. Franklin, N.L. Forsyth, J.S. (1953), "The interpretation of Minimum Reflux Conditions in Multi-Component Distillation" *Trans. IChemE*, Vol. **31**, 1953.
12. Grossmann, I. E. and caballero J.A. (2002), "Structural considerations and modeling in the synthesis of heat integrated thermally coupled distillation sequences", *Chemical Engineering Journal*, **28**, 317-372.
13. Glinos, K.N. and Nikolaides, I.P. and Malone, M.F. (1986) "New complex column arrangements for ideal distillation", *Ind. Eng. Chem. Process Des. Dev.*, 1986, vol. **25**, no 3, pp 694-699
14. Gordon, L.M. (1986), "Simple Optimization for Dual Composition Control", *Hydrocarbon Processing*, June 1986, pp 59-62.
15. Halvorsen, I.J. Skogestad, S. and Serra M. (1996), "Evaluation of self-optimizing control structures for an integrated petlyuk distillation column", *Journal of Process Control*, **13**, 418-424.
16. Halvorsen, S. and Skogestad, S. (2003), "Minimum Energy Consumption in Multicomponent Distillation. 1. *Vmin* Diagram for a Two-Product Column", *Ind. Eng. Chem. Res.*, **43**, 596-604.
17. Hernandez, S. and Gimenez, A. (1997), "Design of energy - efficient petlyuk systems", *Computers and Chemical Engineering*, **23**, 1005-1010.
18. Hernandez, S. and Jimenez, A. (1999), "Controllability Analysis of Thermally Coupled Distillation Systems", *Ind. Eng. Chem. Res.*, **38**, 3957-3963.
19. Kim, Y.H. (2001), "Structural design and operation of a fully thermally coupled distillation column", *Chemical Engineering Journal*, **85**, 289-301.
20. Kim, Y.H. (2002), "Rigorous design of extended fully thermally coupled distillation columns", *Chemical Engineering Journal*, **89**, 89-99.
21. Kim, Y.H. (2005), "Evaluation of three-column distillation system for ternary separation", *Chemical Engineering and Processing*, **44**, 1008-1016.
22. King, C.J. (1980), "Separation Processes", McGraw-Hill, Chemical Engineering series, New York, 2nd edition 1980.
23. Koehler, J. and Poellmann, P. and Blass, E., "A Review on Minimum Energy Calculations for Ideal and Non ideal Distillation", *Ind. Eng. Chem. Res.*, Vol. **34**, no 4, pp 1003-1020, 1995.

24. Neri, B. Mazzotti, M. Storti, G. Morbidelli, M., "Multicomponent Distillation Design Through Equilibrium Theory", *Ind. Eng. Chem. Res.* Vol. **37**, pp 2250-2270, 1998.
25. Segovia-Hernandez, J.G. and Hernandez, S., Jimenez, A. (2005), "Analysis of dynamic properties of alternative sequences to the Petlyuk column", *Computers and Chemical Engineering*, **29**, 1389-1399.
26. Serra, M., Espuna, A. and Puigjaner, L. (1999), "Control and optimization of the divided wall column (petlyuk distillation column)", *Chemical Engineering and Processing*, **38**,549-562.
27. Shiras, R.N., Hansson, D.N. and Gibson, C.H., "Calculation of Minimum Reflux in Distillation Columns" *Industrial and Engineering Chemistry*, Vol. **42**, no 18, p 871-876, 1950.
28. Skogestad, S. and Halvorsen, I. J. (1999), "Optimal operation of Petlyuk distillation: steady-state behavior", *Journal of Process Control*, **9**,407-424.
29. Skogestad, S. and Skogestad, S. (2004) "Shortcut Analysis of Optimal Operation of Petlyuk Distillation", *Ind. Eng. Chem.Res*, **43**, 3994-3999.
30. Underwood, A.J.V. et. al. (1945), "Fractional Distillation of Ternary Mixtures", Part I. *J. Inst. Petroleum*, **31**, 111-118, 1945.
31. Underwood, A.J.V. et. al. (1946a), "Fractional Distillation of Ternary Mixtures", Part II. *J. Inst. Petroleum*, **32**, 598-613, 1946
32. Underwood, A.J.V. (1946b), "Fractional Distillation of Multi-Component Mixtures - Calculation of Minimum reflux Ratio", *Inst. Petroleum*, **32**, 614-626, 1946
33. Underwood, A.J.V. (1948), "Fractional Distillation of Multi-Component mixtures", *Chemical Engineering Progress*, Vol-**44**, no.-8, 1948.
34. Wachter, J.A. and Ko, T.K.T. and Andres, R.P., (1988), "Minimum Reflux Behavior of Complex Distillation Columns", *AIChE J.* Vol. **34**, no 7, 1164-84, 1988

APPENDIX-A

Table A.1 Vapor Flow rates at the Peaks and Knots in the V_{min} – diagram at the different composition of the saturated liquid feed.

$\alpha[4.20, 1.86, 1.00]$					
$z[z_A, z_B, z_C]$	P_0	P_{AB}	P_{BC}	P_{AC}	P_1
[0.1, 0.4, 0.5]	$\Theta_A=3.543$		$\Theta_B=1.325$		
V_{Tmin}	0	0.6393	1.5367	0.5203	0
D	0	0.10	0.50	0.2076	1
[0.2, 0.2, 0.6]	$\Theta_A=2.9272$		$\Theta_B=1.4738$		
V_{Tmin}	0	0.65996	1.2714	0.56646	0
D	0	0.20	0.40	0.2536	1
[0.3, 0.3, 0.4]	$\Theta_A=2.74067$		$\Theta_B=1.28512$		
V_{Tmin}	0	0.8634	1.4029	0.6931	0
D	0	0.30	0.60	0.3806	1
[0.4, 0.4, 0.2]	$\Theta_A=2.639$		$\Theta_B=1.128$		
V_{Tmin}	0	1.0762	1.5633	0.8198	0
D	0	0.4	0.8	0.5074	1
[0.7, 0.2, 0.1]	$\Theta_A=2.138$		$\Theta_B=1.071$		
V_{Tmin}	0	1.4255	1.4111	1.0660	0
D	0	0.70	0.90	0.7537	1
[0.85, 0.1, 0.05]	$\Theta_A=2.979$		$\Theta_B=1.037$		
V_{Tmin}	0	1.6074	1.3547	1.1891	0
D	0	0.85	0.95	0.8768	1

Table A.2 Vapor Flow rates at the Peaks and Knots in the V_{min} – diagram at the different feed conditions.

$\alpha[4.20, 1.86, 1.00]$ and $z[0.3, 0.3, 0.4]$							
Feed Condition (q-value)	Θ_A	Flow rates	P_0	P_{AB}	P_{BC}	P_{AC}	P_1
	Θ_B						
Cold Feed as Liquor $q = 1.5$	2.4507	V_{Tmin}	0	0.7203	1.2983	0.5660	-0.5
	1.2224	D	0	0.30	0.60	0.349	1
Saturated Liquid $q = 1$	2.74067	V_{Tmin}	0	0.8634	1.4029	0.6931	0
	1.28512	D	0	0.30	0.60	0.3806	1
Feed Partly Vapor $q = 0.8$	2.8838	V_{Tmin}	0	0.9573	1.4636	0.7769	0.2
	1.3165	D	0	0.30	0.60	0.3993	1
Saturated Vapor $q = 0$	3.3794	V_{Tmin}	0	1.5355	1.8644	1.3125	1
	1.4626	D	0	0.30	0.60	0.4821	1
Superheated Vapor $q = -0.25$	3.4821	V_{Tmin}	0	1.7551	2.0412	1.5242	1.25
	1.5054	D	0	0.30	0.60	0.5014	1